

Landau-Lifschitz magnets: exact thermodynamics and transport

Alvise Bastianello,^{1,2} Žiga Krajnik,³ and Enej Ilievski⁴

¹Technical University of Munich, TUM School of Natural Sciences, Physics Department, 85748 Garching, Germany

²Munich Center for Quantum Science and Technology (MCQST), Schellingstr. 4, 80799 München, Germany

³Department of Physics, New York University, 726 Broadway, New York, NY 10003, USA

⁴Faculty for Mathematics and Physics, University of Ljubljana, Jadranska ulica 19, 1000 Ljubljana, Slovenia

The classical Landau–Lifshitz equation – the simplest model of a ferromagnet – provides an archetypal example for studying transport phenomena. In one-spatial dimension, integrability enables the classification of the spectrum of linear and nonlinear modes. An exact characterization of finite-temperature thermodynamics and transport has nonetheless remained elusive. We present an exact description of thermodynamic equilibrium states in terms of interacting modes. This is achieved by retrieving the classical Landau–Lifshitz model through the semiclassical limit of the integrable quantum spin- S anisotropic Heisenberg chain at the level of the thermodynamic Bethe ansatz description. In the axial regime, the mode spectrum comprises solitons with unconventional statistics, whereas in the planar regime we additionally find two special types of modes of radiative and solitonic type. The obtained framework paves the way for analytical study of unconventional transport properties: as an example we study the finite-temperature spin Drude weight, finding excellent agreement with Monte Carlo simulations.

Introduction — A quantitative understanding of macroscopic phenomena in interacting many-body systems is a central goal of theoretical and experimental physics. However, strong interactions make perturbative calculations unreliable. To make progress, one has to identify appropriate collective degrees of freedom. An emblematic example of this paradigm are solitons, referring to stable particle-like coherent field excitations, found across various domains of physics including shallow water waves [1], gravity [2], cold-atom gases [3–5], magnets [6, 7] and many more. Since the density of excited solitons is highly suppressed at low temperatures, it has been proposed that thermodynamic properties of the model can be accessed by treating it as a dilute gas, assuming solitons behave as well-separated quasiparticles [8] – giving birth to the phenomenological *soliton-gas approach* [9–14].

While initially devised only as an approximate technique for capturing physics at low temperature, it was later argued that for integrable models the soliton-gas formulation should provide an accurate description even at finite temperature [9]. However, while the inverse scattering method [15–17] permits an analytic solution of the initial-value problem, a rigorous microscopic derivation of thermodynamics remained an unsolved challenge. Recent analytical works [18–21] use the distribution of soliton parameters (classical actions) as a phenomenological input without establishing any connection to standard thermodynamic state functions. Important progress has so far been made in certain special cases, including models that only feature radiative modes, such as the sinh-Gordon theory and defocusing non-linear Schrödinger equation [22], or a single soliton species as in the Toda chain [23–26], the KdV equation [27], and the Ablowitz–Ladik model [28, 29]. On the other hand, in generic models such as the sine-Gordon

model, focusing non-linear Schrödinger equation and the Landau-Lifschitz equation [16], the structure of the mode spectrum is more intricate, comprising both radiative modes and solitons of arbitrarily small charge. In the meantime, rapid advances in the manipulation of quantum matter [30, 31] have steered interest towards the study of quantum integrable systems [32–37]. The quantum variant of the soliton-gas approach, known as generalized hydrodynamics (GHD) [38–40] has led to a wide array of exact predictions, both in and out of equilibrium, culminating in an experimental confirmation [41–45].

The recent discovery of anomalous spin transport in quantum integrable magnets has boosted theoretical [46–53] and experimental [54–57] interest. In view of the current incomplete theoretical understanding, numerical simulations play an invaluable role. Unfortunately, the timescales required to reliably capture the late-time dynamics in quantum systems are very often beyond the capabilities of current numerical techniques. This difficulty partly motivates the study of classical spin chains [58–65]. Despite many attempts to employ the soliton-gas approach to study equilibrium properties of classical integrable spin chains [66, 67] (see also the related works [68–71]), numerous inconsistencies and controversies [72] remain unresolved, suggesting that the approach might be fundamentally flawed. We thus currently face a dichotomy: numerical simulations are barely catching up with analytical predictions in quantum models, whereas the opposite is true for classical systems. In this Letter we resolve this impasse by deriving the exact thermodynamics and hydrodynamics of the classical Landau-Lifschitz (LL) model. This result paves the way for studying dynamical properties of integrable magnets by bridging the gap between theoretical understanding and numerical methods.

The model— Time-evolution of the one-dimensional classical Landau-Lifschitz magnet is generated by the Hamiltonian

$$H_{\text{LL}} = \frac{1}{2} \int_{\mathbb{R}} dx [(\partial_x \mathbf{S})^2 + \Delta(1 - (S^3)^2)], \quad (1)$$

where the spin field $\mathbf{S}(x) = (S^1(x), S^2(x), S^3(x))$, normalized to unity $\mathbf{S} \cdot \mathbf{S} = 1$, obeys the Lie-Poisson brackets $\{S^a(x), S^b(y)\} = \mathcal{E} \epsilon_{abc} S^c(x) \delta(x - y)$ and $\Delta \in \mathbb{R}$ is the anisotropy. Here \mathcal{E} is a free parameter used to set the timescale in the equation of motion $d\mathbf{S}/dt = \{\mathbf{S}, H\}$. We pick $\mathcal{E} = 2$ for reasons that will be clarified later on. The third component of total magnetization, $M^3 \equiv \int dx S^3(x)$, is conserved in time. In the easy-axis regime $\Delta > 0$, the lowest energy configurations are doubly-degenerate ferromagnetic vacua parallel to the anisotropy axis, while the easy-plane phase $\Delta < 0$ there is a $U(1)$ -degeneracy of ferromagnetic ground states polarized in the plane normal to the third axis. The model admits an integrable lattice discretization [16], the lattice Landau-Lifschitz (LLL) model, $H_{\text{LLL}} = -2 \sum_{\ell} \log \Phi_{\ell, \ell+1}$ with

$$\Phi_{\ell, \ell+1} = \Upsilon(S_{\ell}^3) \Upsilon(S_{\ell+1}^3) (S_{\ell}^1 S_{\ell+1}^1 + S_{\ell}^2 S_{\ell+1}^2) + U(1) U\left(\frac{1}{2}(S_{\ell}^3 + S_{\ell+1}^3)\right) - U\left(\frac{1}{2}(S_{\ell}^3 - S_{\ell+1}^3)\right), \quad (2)$$

with auxiliary functions $U(y) \equiv \cosh(\varrho_{\text{ea}} y)$ and $\Upsilon(y) \equiv \sqrt{(U(1) - U(y))/(1 - y^2)}$, and the easy-axis anisotropy parameter $\varrho_{\text{ea}} \in \mathbb{R}_+$. The easy-plane regime is reached by analytic continuation $\varrho_{\text{ea}} \rightarrow i \varrho_{\text{ep}}$, $\varrho_{\text{ep}} \in [-\pi, \pi]$. The continuum limit, yielding Eq. (1), is recovered at large wavelengths by introducing the lattice spacing a , expanding $\mathbf{S}_{\ell \pm 1} = \mathbf{S}(x) \pm a \partial_x \mathbf{S}(x) + \mathcal{O}(a^2)$, rescaling the interaction as $\varrho = a\sqrt{\Delta}$, and letting $a \rightarrow 0$. Since the field theory is accessible as a limit of the lattice Hamiltonian (2), we subsequently focus our discussion on the lattice model.

Any spin configuration that at spatial infinity decays to the ferromagnetic vacuum exponentially fast can be uniquely decomposed in terms of delocalized radiative modes and localized solitons (defined above the vacuum) by means of the inverse scattering method (ISM) [16], see Fig. 1(a) for a pictorial representation. A downside of the ISM is that it does not, at least directly, describe finite-energy density configurations. It has nonetheless been assumed that the ISM's excitation spectrum can be used to compute exact thermodynamic properties using the soliton-gas phenomenology [66, 67]. However, whether *i*) these modes truly form an (over)complete set of degrees of freedom, and *ii*) how to obtain their statistical weights has remained an open question. Since such difficulties do not arise in quantum models, one can use the thermodynamic Bethe ansatz [73] to infer the complete excitation spectrum in classical systems, including the correct statistical weights, in a systematic fashion.

In this work, our strategy is to retrieve the Landau-Lifschitz model via the large-spin limit of *integrable* quan-

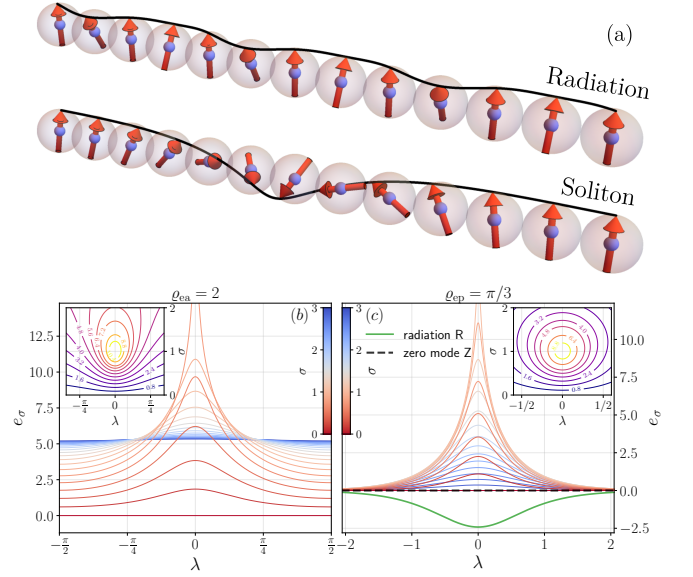


FIG. 1. Landau-Lifschitz excitations.— (a) The inverse scattering method decomposes a spin configuration in terms of delocalized radiation (akin to spin-waves) and localized solitons as the fundamental excitations above the ferromagnetic vacuum. In the thermodynamic limit the mode structure depends on the regime. (b) The easy-axis regime supports a continuous family of solitons whose energy $e_{\sigma}(\lambda)$ is sharply peaked at $(\lambda, \sigma) = (0, 1)$ (see text for details). (c) The easy-plane regime supports two additional types of modes: radiation R with negative energy and a zero mode Z with vanishing energy. Insets of Panels (b), (c) show energy contours in the two regimes.

tum spin- S chains [74–78]. Such a limit has been previously worked out at the algebraic level [61, 79] and (for the isotropic model) at the level of equations of motion [80]. Building on recent developments in understanding semiclassical limits of integrable quantum models [81–86], our approach is to take the limit at the level of thermodynamic states. While a recent study [50] has already pointed out that so-called giant magnons of the quantum Heisenberg chain manifest as classical solitons, the outlined method is fully general and permits an exact mapping between quantum and classical degrees of freedom.

We proceed by summarizing our key results. We focus on the most salient physical features while leaving most of the technical details, including the derivations, to the Supplementary Material (SM) [87]. Our analysis confirms the intuitive view that thermodynamics of the LL model can be described as a gas of interacting solitons and radiative modes, with the important caveat that their statistics are unconventional and depend on the regime.

Thermodynamics of integrable models.— We briefly introduce the setting of TBA and define thermodynamic state functions (for more details, see SM [87])

or the standard literature [73]). Individual modes (excitations) are assigned a type (species) index “ I ”. The associated (bare) energy and momentum are denoted by $e_I(\lambda)$ and $p_I(\lambda)$ respectively, conveniently parametrized in terms of the rapidity λ . In spin chains, an excitation of type I carries m_I quanta of magnetization relative to the ferromagnetic vacuum. On the other hand, the two degrees of freedom of classical magnetic solitons (e.g. magnetization and velocity) take *continuous* values. For compactness, we introduce an implicit notation for the scalar product $a_I \circ b_I$ and convolution $a_I \star b_I$, evaluated over the rapidity domain for any two quantities a_I and b_I ascribed to specie I , while simultaneously adopting summation over all the repeated indexes I (integration when I has a continuous range, see SM [87] for details). We specialize our study to grand-canonical equilibrium ensembles with partition sum $Z(\beta, \mu) \equiv \int d\Omega e^{-\beta H + \mu(M^3 - M_{\text{vac}}^3)}$ (normalized by $Z(0, 0) = 1$), where M_{vac}^3 denotes the average of M^3 in the ferromagnetic vacuum and $d\Omega$ is the phase-space volume element.

Gibbs ensembles, or more generally generalized Gibbs ensembles [88], can be understood as macrostates parametrized by rapidity densities ρ_I , describing by a finite-density gas of interacting modes. The available phase space for each mode, given by the total state density $\rho_I^t = \frac{\kappa_I}{2\pi} (\partial_\lambda p_I)^{\text{dr}}$ with $\kappa_I = \text{sign}[\partial_\lambda p_I]$, gets renormalized by interactions. Accordingly, an arbitrary function g_I is dressed, $g_I \mapsto g_I^{\text{dr}}$, by solving the *linear* (Fredholm) integral equation $g_I^{\text{dr}} + T_{I,I'} \star (\kappa_I \vartheta g_I^{\text{dr}})_{I'} = g_I$ where $T_{I,I'}$ encodes the effect of interaction among the species of type I and I' (related to the time delay [89, 90] or phase shift [91] incurred by scattering), while the occupation (filling) fraction is defined as $\vartheta_I \equiv \rho_I / \rho_I^t$.

Equations of state are inferred by minimizing the free energy $F = \beta \langle H \rangle - \mu (\langle M^3 \rangle - M_{\text{vac}}^3) - \mathcal{S}$, where the entropy \mathcal{S} is given by summing over all modes with appropriate statistical weights $s_I = s_I(\vartheta_I)$. The entropy density is thus $s \equiv \lim_{L \rightarrow \infty} (\mathcal{S}/L) = \rho_I^t \circ s_I$, and the spectral resolution of the free energy density $f = \lim_{L \rightarrow \infty} (F/L)$ accordingly reads [87], $f = \frac{1}{2\pi} \kappa_I \partial_\lambda p_I \circ \mathcal{F}_I$, with $\mathcal{F}_I(\vartheta_I) \equiv \vartheta_I s'_I(\vartheta_I) - s_I(\vartheta_I)$. Mode occupations ϑ_I satisfy nonlinear integral equations

$$s'_I(\vartheta_I) = \beta e_I + \mu m_I - T_{I,I'} \star \kappa_{I'} \mathcal{F}_{I'}(\vartheta_{I'}), \quad (3)$$

where $s'_I(\vartheta) = \frac{ds_I(\vartheta)}{d\vartheta}$. The functional form of statistical factors s_I discerns the nature of quasiparticle modes: typically in quantum models, including spin chains, one finds the Fermi-Dirac statistics $s_{\text{FD}}(\vartheta) = -\vartheta \log \vartheta - (1 - \vartheta) \log(1 - \vartheta)$ [73]. By contrast, in classical systems one usually encounters radiation $s_{\text{Rad}}(\vartheta) = \log \vartheta$ [82, 83] with Rayleigh-Jeans statistics, or solitons $s_{\text{Sol}}(\vartheta) = \vartheta(1 - \log \vartheta)$ [24, 25, 27] with the associated Boltzmann weight. As detailed out in the remainder of the paper, the LL model evades this simple description; we find the model features solitons with unorthodox (renormalized) statistical weights alongside (depending on the regime of

anisotropy) a part of the magnon (radiative) spectrum and exceptional (zero-energy) modes.

Completeness of classical TBA equations.—

To establish completeness of the derived classical TBA equations, we show that no relevant classical mode has been lost upon taking the semiclassical limit. In infinite-temperature Gibbs ensemble, this task can be achieved analytically: using that the partition sum factorizes, the free energy density $f(\mu)$ and the average magnetization, $\langle S^3 \rangle = -1/\mu + \coth \mu$, can be computed directly. To validate our thermodynamics, we analytically retrieve these results from the TBA equations [87]. Additionally, we find excellent agreement with numerical simulations (Fig. 2 and SM [87]) at finite temperatures.

Drude weight.— Owing to the presence of long-lived ballistically propagating modes, integrable systems generically possess divergent conductivities signalled by finite Drude weights. We focus on the spin Drude weight, $\mathcal{D} = \lim_{t \rightarrow \infty} \int dx \langle j(x, t) j(0, 0) \rangle_c$ where the spin current density $j(x, t)$ is defined via $\partial_t S^3(x, t) + \partial_x j(x, t) = 0$, that admits the following mode resolution [92–94] (see also SM [87])

$$\mathcal{D} = \rho_I w_I \circ (m_I^{\text{dr}} v_I^{\text{eff}})^2, \quad (4)$$

where $w_I(\vartheta_I) \equiv -1/[\vartheta_I s''_I(\vartheta_I)]$ accounts for the mode statistics and the effective velocity is $v_I^{\text{eff}} \equiv (\partial_\lambda e_I)^{\text{dr}} / (\partial_\lambda p_I)^{\text{dr}}$. The latter identification is sensitive to the choice of time scale in the equation of motion, our choice $\mathcal{E} = 2$ ensures its validity, see SM [87]. It is worth emphasizing that Drude weights are genuine dynamical quantities that cannot be extracted from any thermodynamic potential. Therefore, aside from their physical significance, computation of the spin Drude weight also serves as an important benchmark of our hydrodynamic equations.

Easy-axis regime.— We first inspect the easy-axis regime of the lattice Hamiltonian (2). More details, including the scaling to the continuum Hamiltonian (1), can be found in SM [87]. In this regime, rapidity occupies a compact domain $\lambda \in [-\pi/2, \pi/2]$, and the mode spectrum comprises solely from solitons with bare energy $e_\sigma(\lambda)$, labeled by λ and a *continuous* internal variable $\sigma \in \mathbb{R}_+$ associated with magnetization $m_\sigma = 2\sigma$ and with positive parity $\kappa_\sigma = 1$. A typical dispersion law is shown in Fig. 1(b). The power-law singularity at $(\sigma, \lambda) = (1, 0)$ is a consequence of the logarithmic interaction in Eq.(2). Solitons acquire *renormalized* Boltzmann weights

$$s_\sigma(\vartheta_\sigma) = s_{\text{Sol}}(\vartheta_\sigma) - \sigma^{-2} - \vartheta_\sigma \log \sigma^2. \quad (5)$$

Although the form of s_σ affects the filling fraction (3), we note that the additional terms (constant or linear in ϑ_σ) do not affect the function w_I appearing in the Drude weight (4). The kinematic data retrieved by taking the semiclassical limit is compatible with expressions derived using the ISM (see SM [87] for explicit expressions).

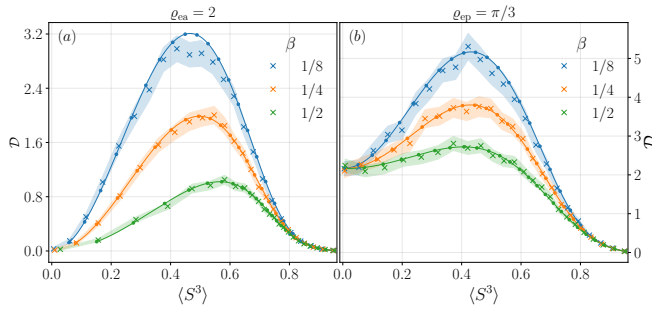


FIG. 2. Spin Drude weights computed from classical TBA equations (circles, solid lines as a guide to the eye), shown for three values of β in (a) the easy-axis regime with $\varrho_{ea} = 2$ and (b) the easy-plane regime with $\varrho_{ep} = \pi/3$, compared to numerical results (crosses, with shaded regions showing two standard deviation confidence intervals). Simulation parameters: system size $L = 2 \times 10^3$, number of samples $N = 2 \times 10^3$, time-step $\tau = 0.03$, see Ref. [61] for details.

In Fig. 2 (a) we show the Drude weight for a representative interaction $\varrho_{ea} = 2$ and for different temperatures, obtained by numerically solving the classical TBA equations and independently by performing Monte-Carlo simulations [95, 96], see also SM [87]. The divergence of the bare energy $e_\sigma(\lambda)$ at $(\sigma, \lambda) = (1, 0)$, see Fig. 1(b), causes a singularity in the effective velocity v^{eff} . The singularity is balanced by a zero of the filling function $\vartheta_\sigma(\lambda) \propto e^{-\beta e_\sigma(\lambda)} \propto ((\sigma - 1)^2 \varrho_{ea}^2 + 4\lambda^2)^{2\beta}$, rendering the Drude weight finite. However, this ‘damping’ mechanism diminishes with decreasing β , resulting in a logarithmic divergence of the Drude weight at high temperatures, $D \propto \log \beta^{-1}$ [87].

Easy-plane regime.— Remarkably, in the easy-plane regime there appear *three* distinct types of quasiparticles (above the ferromagnetic vacuum): a continuum of magnetic solitons with renormalized statistics (analogous to those in the easy-axis regime) and $\sigma \in [0, \pi/\varrho_{ep}]$, a single radiative mode R with $m_R = 2$ and renormalized entropy $s_R(\vartheta_R) = s_{\text{Rad}}(\vartheta_R) + 1 + \log(\varrho_{ep}/\pi)$ and, finally, a special type of soliton mode Z with no bare energy nor momentum, $e_Z = \partial_\lambda p_Z = 0$, characterized by finite magnetization $m_Z = 2\pi/\varrho_{ep}$ and renormalized entropy weight $s_Z(\vartheta_Z) = s_{\text{Sol}}(\vartheta_Z) - \vartheta_Z \log(\pi/\varrho_{ep})$. Solitons have positive parity $\kappa_\sigma = 1$ and $\kappa_Z = 1$, in contrast with the radiative mode $\kappa_R = -1$. The dispersion laws of these modes are represented in Fig. 1(c), featuring the same type of singularity found in the easy-axis regime, causing a logarithmically divergent Drude weight in the high-temperature limit. The rapidities in the planar regime span the whole real line $\lambda \in \mathbb{R}$, the explicit dispersion laws and scattering kernels are reported in SM [87]. In Fig. 2(b) we compare the Drude weight (4) with our Monte Carlo numerical data for $\varrho_{ep} = \pi/3$.

The spin-waves limit.— Small fluctuations of the ferromagnetic vacuum are resolved in terms of non-

interacting delocalized spin-waves, i.e. solutions of the linearized dynamics. Given that the statistics of these excitations corresponds to canonical radiative modes, one may ask whether our description in terms of unconventional solitons is compatible with the spin wave picture. It turns out that in the easy-axis regime, spin-waves are recovered from summing over σ , i.e. the soliton continuum. The same holds for the positive-energy radiation branch in the easy-plane regime. By contrast, the radiative branch with negative energy must be included in the TBA as an independent mode. Note that Z modes carry finite magnetization and are effectively eliminated at low densities. spin-waves thermodynamics thus emerges from the full TBA equations, see SM [87] for a straightforward but lengthy derivation.

Discussion.— By performing the semiclassical limit of the integrable quantum spin- S chain within the framework of the thermodynamic Bethe ansatz, we have obtained the exact thermodynamics and hydrodynamics of the classical Landau–Lifshitz spin chain, thereby establishing validity of the soliton-gas description, but with several important nuances.

Our approach uncovered several unexpected features. Firstly, in the easy-axis regime we found a spectrum of solitons with modified Boltzmann statistics, while radiative modes (spin-waves) do not show up as independent modes and can instead be seen as a condensate of wide solitons with small amplitude. The easy-plane regime is even more unconventional: apart from solitons, the spectrum of modes explicitly includes the negative energy spin-waves branch and localized zero-energy modes, both of which are responsible for ballistic spin transport at half-filling. Our solution thus explains this peculiar feature of spin transport in the classical setting.

A number of questions remain unanswered. Most prominently, it is still unclear whether the easy-plane regime of the model hosts additional quasilocal charges with odd parity under spin reversal, as conjectured previously in [97]. Evidently, there is no room for classical counterparts of ‘Z-charges’ [98–101], since there can be at most L functionally independent conserved quantities in mutual involution in a phase space of dimension $2L$. There might nonetheless exist hidden nonabelian quasilocal charges which we are presently unable to rule out. A viable alternative scenario is the breakdown of the hydrodynamic (Suzuki–Mazur) projection [101–104] attributed to a lack of causality (presently caused by the logarithmic singularity in the energy density).

Our results open the doors for a new understanding of unconventional transport properties in integrable magnets such as, for example, the onset of spin superdiffusion at the isotropic point and its conjectured connection to the universality class of the Kadar–Parisi–Zhang equation: while the dynamical exponent and scaling function are by now firmly established, [47, 48, 51, 58, 59, 97, 105, 106], the spin-current’s fluctuations [62, 63, 107] are dis-

cernibly distinct. The computation of the full counting statistics of charge transport [108–110] in classical integrable magnets (which employs TBA equations) might provide important new insights. There remain other interesting questions such as e.g. a hydrodynamic description of gauge modes associated with the vacuum polarization at the isotropic point [111] and the study of thermalization in the presence of integrability breaking [112] with many species of quasiparticles. Addressing these questions requires both extensive numerical benchmarks and a fully-fledged analytical toolbox. The present work makes the classical Landau–Lifschitz model an ideal playground for realizing this program.

Data and code availability— Raw data and working codes are available on Zenodo [113].

Acknowledgments— We thank Tomaž Prosen, Oleksandr Gamayun, Takato Yoshimura and Jacopo De Nardis for useful discussions and comments on the manuscript. AB acknowledges support from the Deutsche Forschungsgemeinschaft (DFG, German Research Foundation) under Germany’s Excellence Strategy–EXC–2111–390814868. ŽK is supported by the Simons Foundation via a Simons Junior Fellowship grant 1141511. EI is supported by the Slovenian Research Agency (ARIS) grants P1-0402 and N1-0243.

-
- [1] M. Remoissenet, *Waves called solitons: concepts and experiments* (Springer Science & Business Media, 2013).
 - [2] E. Verdaguer, *Gravitational Solitons. Cambridge Monographs on Mathematical Physics* (Cambridge University Press, 2001).
 - [3] B. Eiermann, T. Anker, M. Albiez, M. Taglieber, P. Treutlein, K.-P. Marzlin, and M. K. Oberthaler, Bright bose-einstein gap solitons of atoms with repulsive interaction, *Phys. Rev. Lett.* **92**, 230401 (2004).
 - [4] O. Morsch and M. Oberthaler, Dynamics of bose-einstein condensates in optical lattices, *Rev. Mod. Phys.* **78**, 179 (2006).
 - [5] S. Lannig, C.-M. Schmied, M. Prüfer, P. Kunkel, R. Strohmaier, H. Strobel, T. Gasenzer, P. G. Kevrekidis, and M. K. Oberthaler, Collisions of three-component vector solitons in bose-einstein condensates, *Phys. Rev. Lett.* **125**, 170401 (2020).
 - [6] A. Farolfi, D. Trypogeorgos, C. Mordini, G. Lamporesi, and G. Ferrari, Observation of magnetic solitons in two-component bose-einstein condensates, *Phys. Rev. Lett.* **125**, 030401 (2020).
 - [7] X. Chai, D. Lao, K. Fujimoto, R. Hamazaki, M. Ueda, and C. Raman, Magnetic solitons in a spin-1 bose-einstein condensate, *Phys. Rev. Lett.* **125**, 030402 (2020).
 - [8] J. A. Krumhansl and J. R. Schrieffer, Dynamics and statistical mechanics of a one-dimensional model hamiltonian for structural phase transitions, *Phys. Rev. B* **11**, 3535 (1975).
 - [9] J. F. Currie, J. A. Krumhansl, A. R. Bishop, and S. E. Trullinger, Statistical mechanics of one-dimensional solitary-wave-bearing scalar fields: Exact results and ideal-gas phenomenology, *Phys. Rev. B* **22**, 477 (1980).
 - [10] N. Theodorakopoulos, Ideal-gas approach to the statistical mechanics of integrable systems: The sine-gordon case, *Phys. Rev. B* **30**, 4071 (1984).
 - [11] K. Sasaki, Soliton-breather approach to classical sine-gordon thermodynamics, *Phys. Rev. B* **33**, 2214 (1986).
 - [12] S. Sachdev and A. P. Young, Low temperature relaxational dynamics of the ising chain in a transverse field, *Phys. Rev. Lett.* **78**, 2220 (1997).
 - [13] K. Damle and S. Sachdev, Universal relaxational dynamics of gapped one-dimensional models in the quantum sine-gordon universality class, *Phys. Rev. Lett.* **95**, 187201 (2005).
 - [14] M. Kormos and G. Zaránd, Quantum quenches in the sine-gordon model: A semiclassical approach, *Phys. Rev. E* **93**, 062101 (2016).
 - [15] M. J. Ablowitz and H. Segur, *Solitons and the inverse scattering transform* (SIAM, 1981).
 - [16] L. D. Faddeev and L. A. Takhtajan, *Hamiltonian Methods in the Theory of Solitons* (Springer Berlin Heidelberg, 1987).
 - [17] S. Novikov, S. V. Manakov, L. P. Pitaevskii, and V. E. Zakharov, *Theory of solitons: the inverse scattering method* (Springer Science & Business Media, 1984).
 - [18] G. El, The thermodynamic limit of the whitham equations, *Physics Letters A* **311**, 374 (2003).
 - [19] V. E. Zakharov, Turbulence in integrable systems, *Studies in Applied Mathematics* **122**, 219 (2009), <https://onlinelibrary.wiley.com/doi/pdf/10.1111/j.1467-9590.2009.00430.x>.
 - [20] G. A. El, Soliton gas in integrable dispersive hydrodynamics, *Journal of Statistical Mechanics: Theory and Experiment* **2021**, 114001 (2021).
 - [21] P. Suret, S. Randoux, A. Gelash, D. Agafontsev, B. Doyon, and G. El, Soliton gas: Theory, numerics and experiments (2023), arXiv:2304.06541 [nlin.SI].
 - [22] R. K. Bullough, D. J. Pilling, and J. Timonen, Quantum and classical statistical mechanics of the sinh-gordon equation, *Journal of Physics A: Mathematical and General* **19**, L955 (1986).
 - [23] N. Theodorakopoulos, Nontopological thermal solitons in isotropic ferromagnetic lattices, *Phys. Rev. B* **52**, 9507 (1995).
 - [24] X. Cao, V. B. Bulchandani, and H. Spohn, The gge averaged currents of the classical toda chain, *Journal of Physics A: Mathematical and Theoretical* **52**, 495003 (2019).
 - [25] B. Doyon, Generalized hydrodynamics of the classical Toda system, *Journal of Mathematical Physics* **60**, 073302 (2019), https://pubs.aip.org/aip/jmp/article-pdf/doi/10.1063/1.5096892/16061795/073302.1_online.pdf.
 - [26] V. B. Bulchandani, X. Cao, and J. E. Moore, Kinetic theory of quantum and classical toda lattices, *Journal of Physics A: Mathematical and Theoretical* **52**, 33LT01 (2019).
 - [27] T. Bonnamain, B. Doyon, and G. El, Generalized hydrodynamics of the kdv soliton gas, *Journal of Physics A: Mathematical and Theoretical* **55**, 374004 (2022).
 - [28] H. Spohn, Hydrodynamic equations for the Ablowitz–Ladik discretization of the nonlinear Schrödinger equation, *Journal of Mathematical Physics* **63**, 033305 (2022), <https://pubs.aip.org/aip/jmp/article->

- pdf/doi/10.1063/5.0075670/16560227/033305_1_online.pdf.
- [29] A. Brollo and H. Spohn, Particle scattering and fusion for the ablowitz-ladik chain (2024), arXiv:2404.07095 [cond-mat.stat-mech].
 - [30] I. Bloch, J. Dalibard, and W. Zwerger, Many-body physics with ultracold gases, *Rev. Mod. Phys.* **80**, 885 (2008).
 - [31] I. Bloch, J. Dalibard, and S. Nascimbène, Quantum simulations with ultracold quantum gases, *Nature Physics* **8**, 267 (2012).
 - [32] T. Kinoshita, T. Wenger, and D. S. Weiss, A quantum newton's cradle, *Nature* **440**, 900 (2006).
 - [33] E. Haller, M. Gustavsson, M. J. Mark, J. G. Danzl, R. Hart, G. Pupillo, and H.-C. Nägerl, Realization of an excited, strongly correlated quantum gas phase, *Science* **325**, 1224 (2009), <https://www.science.org/doi/pdf/10.1126/science.1175850>.
 - [34] T. Langen, S. Erne, R. Geiger, B. Rauer, T. Schweigler, M. Kuhnert, W. Rohringer, I. E. Mazets, T. Gasenzer, and J. Schmiedmayer, Experimental observation of a generalized gibbs ensemble, *Science* **348**, 207 (2015), <https://www.science.org/doi/pdf/10.1126/science.1257026>.
 - [35] T. Schweigler, V. Kasper, S. Erne, I. Mazets, B. Rauer, F. Cataldini, T. Langen, T. Gasenzer, J. Berges, and J. Schmiedmayer, Experimental characterization of a quantum many-body system via higher-order correlations, *Nature* **545**, 323 (2017).
 - [36] J. M. Wilson, N. Malvania, Y. Le, Y. Zhang, M. Rigol, and D. S. Weiss, Observation of dynamical fermionization, *Science* **367**, 1461 (2020), <https://www.science.org/doi/pdf/10.1126/science.aaz0242>.
 - [37] X.-W. Guan and P. He, New trends in quantum integrability: recent experiments with ultracold atoms, *Reports on Progress in Physics* **85**, 114001 (2022).
 - [38] O. A. Castro-Alvaredo, B. Doyon, and T. Yoshimura, Emergent hydrodynamics in integrable quantum systems out of equilibrium, *Phys. Rev. X* **6**, 041065 (2016).
 - [39] B. Bertini, M. Collura, J. De Nardis, and M. Fagotti, Transport in out-of-equilibrium xxz chains: Exact profiles of charges and currents, *Phys. Rev. Lett.* **117**, 207201 (2016).
 - [40] A. Bastianello, B. Bertini, B. Doyon, and R. Vasseur, Introduction to the special issue on emergent hydrodynamics in integrable many-body systems, *Journal of Statistical Mechanics: Theory and Experiment* **2022**, 014001 (2022).
 - [41] I. Bouchoule and J. Dubail, Generalized hydrodynamics in the one-dimensional bose gas: theory and experiments, *Journal of Statistical Mechanics: Theory and Experiment* **2022**, 014003 (2022).
 - [42] N. Malvania, Y. Zhang, Y. Le, J. Dubail, M. Rigol, and D. S. Weiss, Generalized hydrodynamics in strongly interacting 1d bose gases, *Science* **373**, 1129 (2021), <https://www.science.org/doi/pdf/10.1126/science.abf0147>.
 - [43] F. Møller, C. Li, I. Mazets, H.-P. Stimming, T. Zhou, Z. Zhu, X. Chen, and J. Schmiedmayer, Extension of the generalized hydrodynamics to the dimensional crossover regime, *Phys. Rev. Lett.* **126**, 090602 (2021).
 - [44] F. Cataldini, F. Møller, M. Tajik, J. a. Sabino, S.-C. Ji, I. Mazets, T. Schweigler, B. Rauer, and J. Schmiedmayer, Emergent pauli blocking in a weakly interacting bose gas, *Phys. Rev. X* **12**, 041032 (2022).
 - [45] L. Dubois, G. Thémèze, F. Nogrette, J. Dubail, and I. Bouchoule, Probing the local rapidity distribution of a 1d bose gas (2023), arXiv:2312.15344 [cond-mat.quant-gas].
 - [46] M. Žnidarič, Spin Transport in a One-Dimensional Anisotropic Heisenberg Model, *Physical Review Letters* **106**, 10.1103/physrevlett.106.220601 (2011).
 - [47] M. Ljubotina, M. Žnidarič, and T. Prosen, Kardar-Parisi-Zhang Physics in the Quantum Heisenberg Magnet, *Physical Review Letters* **122**, 10.1103/physrevlett.122.210602 (2019).
 - [48] E. Ilievski, J. De Nardis, M. Medenjak, and T. Prosen, Superdiffusion in one-dimensional quantum lattice models, *Physical Review Letters* **121**, 10.1103/physrevlett.121.230602 (2018).
 - [49] S. Gopalakrishnan and R. Vasseur, Kinetic Theory of Spin Diffusion and Superdiffusion in XXZ Spin Chains, *Physical Review Letters* **122**, 10.1103/physrevlett.122.127202 (2019).
 - [50] J. De Nardis, S. Gopalakrishnan, E. Ilievski, and R. Vasseur, Superdiffusion from emergent classical solitons in quantum spin chains, *Phys. Rev. Lett.* **125**, 070601 (2020).
 - [51] E. Ilievski, J. D. Nardis, S. Gopalakrishnan, R. Vasseur, and B. Ware, Superuniversality of Superdiffusion, *Physical Review X* **11**, 10.1103/physrevx.11.031023 (2021).
 - [52] V. B. Bulchandani, S. Gopalakrishnan, and E. Ilievski, Superdiffusion in spin chains, *Journal of Statistical Mechanics: Theory and Experiment* **2021**, 084001 (2021).
 - [53] L. Piroli, J. De Nardis, M. Collura, B. Bertini, and M. Fagotti, Transport in out-of-equilibrium xxz chains: Nonballistic behavior and correlation functions, *Phys. Rev. B* **96**, 115124 (2017).
 - [54] P. N. Jepsen, J. Amato-Grill, I. Dimitrova, W. W. Ho, E. Demler, and W. Ketterle, Spin transport in a tunable heisenberg model realized with ultracold atoms, *Nature* **588**, 403 (2020).
 - [55] A. Scheie, N. E. Sherman, M. Dupont, S. E. Nagler, M. B. Stone, G. E. Granroth, J. E. Moore, and D. A. Tennant, Detection of kardar-parisi-zhang hydrodynamics in a quantum heisenberg spin-1/2 chain, *Nature Physics* **17**, 726–730 (2021).
 - [56] D. Wei, A. Rubio-Abadal, B. Ye, F. Machado, J. Kemp, K. Srakaew, S. Hollerith, J. Rui, S. Gopalakrishnan, N. Y. Yao, I. Bloch, and J. Zeiher, Quantum gas microscopy of kardar-parisi-zhang superdiffusion, *Science* **376**, 716 (2022), <https://www.science.org/doi/pdf/10.1126/science.abk2397>.
 - [57] E. Rosenberg et al., Dynamics of magnetization at infinite temperature in a heisenberg spin chain, *Science* **384**, 48–53 (2024).
 - [58] A. Das, M. Kulkarni, H. Spohn, and A. Dhar, Kardar-parisi-zhang scaling for an integrable lattice landaulifshitz spin chain, *Phys. Rev. E* **100**, 042116 (2019).
 - [59] Ž. Krajnik and T. Prosen, Kardar-parisi-zhang physics in integrable rotationally symmetric dynamics on discrete space-time lattice, *Journal of Statistical Physics* **179**, 110 (2020).
 - [60] A. Das, K. Damle, A. Dhar, D. A. Huse, M. Kulkarni, C. B. Mendl, and H. Spohn, Nonlinear fluctuating hydrodynamics for the classical xxz spin chain, *Journal of Statistical Physics* **180**, 238–262 (2019).
 - [61] Ž. Krajnik, E. Ilievski, T. Prosen, and V. Pasquier, Anisotropic Landau-Lifshitz model in discrete space-time, *SciPost Phys.* **11**, 051 (2021).

- [62] Ž. Krajnik, E. Ilievski, and T. Prosen, Absence of normal fluctuations in an integrable magnet, *Phys. Rev. Lett.* **128**, 090604 (2022).
- [63] Ž. Krajnik, J. Schmidt, E. Ilievski, and T. Prosen, Dynamical criticality of magnetization transfer in integrable spin chains, *Phys. Rev. Lett.* **132**, 017101 (2024).
- [64] A. J. McRoberts, T. Bilitewski, M. Haque, and R. Moessner, Domain wall dynamics in classical spin chains: Free propagation, subdiffusive spreading, and soliton emission, *Phys. Rev. Lett.* **132**, 057202 (2024).
- [65] D. Roy, A. Dhar, H. Spohn, and M. Kulkarni, Nonequilibrium spin transport in integrable and non-integrable classical spin chains (2023), arXiv:2306.07864 [cond-mat.stat-mech].
- [66] N. Theodorakopoulos and N. C. Bacalis, Semiclassical solitons and the $s=1/2$ heisenberg model, *Phys. Rev. Lett.* **67**, 3018 (1991).
- [67] N. Theodorakopoulos, Nontopological thermal solitons in isotropic ferromagnetic lattices, *Phys. Rev. B* **52**, 9507 (1995).
- [68] J. Timonen, M. Stirland, D. J. Pilling, Y. Cheng, and R. K. Bullough, Statistical mechanics of the sine-gordon equation, *Phys. Rev. Lett.* **56**, 2233 (1986).
- [69] N.-N. Chen, M. D. Johnson, and M. Fowler, Classical limit of bethe-ansatz thermodynamics for the sine-gordon system, *Phys. Rev. Lett.* **56**, 1427 (1986).
- [70] K. Maki, Classical sine-gordon limit of bethe-ansatz thermodynamics, *Phys. Rev. B* **32**, 3075 (1985).
- [71] S. G. Chung, Thermodynamics of the classical massive-thirring-sine-gordon model, *Phys. Rev. Lett.* **62**, 708 (1989).
- [72] S. G. Chung, Breakdown of the soliton-gas phenomenology for the classical statistical mechanics of the sine-gordon model, *Journal of Physics A: Mathematical and General* **23**, L1241 (1990).
- [73] M. Takahashi, *Thermodynamics of one-dimensional solvable models* (Cambridge University Press, 2005).
- [74] A. N. Kirillov and N. Y. Reshetikhin, Exact solution of the integrable xxz heisenberg model with arbitrary spin. i. the ground state and the excitation spectrum, *Journal of Physics A: Mathematical and General* **20**, 1565 (1987).
- [75] A. N. Kirillov and N. Y. Reshetikhin, Exact solution of the integrable XXZ Heisenberg model with arbitrary spin. II. Thermodynamics of the system, *Journal of Physics A: Mathematical and General* **20**, 1587 (1987).
- [76] P. Kulish, N. Reshetikhin, and E. Sklyanin, Yang-baxter equation and representation theory: I (World Scientific, 1990) pp. 498–508, 0.
- [77] H. Frahm, N.-C. Yu, and M. Fowler, The integrable XXZ Heisenberg model with arbitrary spin: Construction of the Hamiltonian, the ground-state configuration and conformal properties, *Nuclear Physics B* **336**, 396 (1990).
- [78] A. G. Bytsko, On integrable hamiltonians for higher spin xxz chain, *Journal of Mathematical Physics* **44**, 3698–3717 (2003).
- [79] E. K. Sklyanin, Classical limits of the $SU(2)$ -invariant solutions of the Yang-Baxter equation, *Journal of Soviet Mathematics* **40**, 93 (1988).
- [80] F. D. M. Haldane, Excitation spectrum of a generalised heisenberg ferromagnetic spin chain with arbitrary spin, *Journal of Physics C: Solid State Physics* **15**, L1309 (1982).
- [81] A. D. Luca and G. Mussardo, Equilibration properties of classical integrable field theories, *Journal of Statistical Mechanics: Theory and Experiment* **2016**, 064011 (2016).
- [82] A. Bastianello, B. Doyon, G. Watts, and T. Yoshimura, Generalized hydrodynamics of classical integrable field theory: the sinh-Gordon model, *SciPost Phys.* **4**, 045 (2018).
- [83] G. D. V. D. Vecchio, A. Bastianello, A. D. Luca, and G. Mussardo, Exact out-of-equilibrium steady states in the semiclassical limit of the interacting Bose gas, *SciPost Phys.* **9**, 002 (2020).
- [84] R. Koch, J.-S. Caux, and A. Bastianello, Generalized hydrodynamics of the attractive non-linear schrödinger equation, *Journal of Physics A: Mathematical and Theoretical* **55**, 134001 (2022).
- [85] R. Koch and A. Bastianello, Exact thermodynamics and transport in the classical sine-Gordon model, *SciPost Phys.* **15**, 140 (2023).
- [86] A. Bastianello, Sine-gordon model from coupled condensates: A generalized hydrodynamics viewpoint, *Phys. Rev. B* **109**, 035118 (2024).
- [87] Supplementary Material for: TBA of the quantum S-spin chain, spin-waves analysis, details on the semiclassical limits, and overview of numerical methods..
- [88] M. Rigol, V. Dunjko, V. Yurovsky, and M. Olshanii, Relaxation in a completely integrable many-body quantum system: An ab initio study of the dynamics of the highly excited states of 1d lattice hard-core bosons, *Phys. Rev. Lett.* **98**, 050405 (2007).
- [89] B. Doyon, T. Yoshimura, and J.-S. Caux, Soliton gases and generalized hydrodynamics, *Phys. Rev. Lett.* **120**, 045301 (2018).
- [90] B. Doyon, F. Hübner, and T. Yoshimura, New classical integrable systems from generalized $t\bar{T}$ -deformations (2023), arXiv:2311.06369 [cond-mat.stat-mech].
- [91] L. D. Faddeev and L. A. Takhtajan, *Hamiltonian methods in the theory of solitons* (1987).
- [92] B. Doyon and H. Spohn, Drude Weight for the Lieb-Liniger Bose Gas, *SciPost Phys.* **3**, 039 (2017).
- [93] B. Doyon, Exact large-scale correlations in integrable systems out of equilibrium, *SciPost Phys.* **5**, 054 (2018).
- [94] J. D. Nardis, B. Doyon, M. Medenjak, and M. Panfil, Correlation functions and transport coefficients in generalised hydrodynamics, *Journal of Statistical Mechanics: Theory and Experiment* **2022**, 014002 (2022).
- [95] N. Metropolis, A. W. Rosenbluth, M. N. Rosenbluth, A. H. Teller, and E. Teller, Equation of State Calculations by Fast Computing Machines, *The Journal of Chemical Physics* **21**, 1087 (2004), https://pubs.aip.org/aip/jcp/article-pdf/21/6/1087/8115285/1087_1.online.pdf.
- [96] W. K. Hastings, Monte Carlo sampling methods using Markov chains and their applications, *Biometrika* **57**, 97 (1970), <https://academic.oup.com/biomet/article-pdf/57/1/97/23940249/57-1-97.pdf>.
- [97] T. Prosen and B. Žunkovič, Macroscopic diffusive transport in a microscopically integrable hamiltonian system, *Phys. Rev. Lett.* **111**, 040602 (2013).
- [98] T. c. v. Prosen, Open xxz spin chain: Nonequilibrium steady state and a strict bound on ballistic transport, *Phys. Rev. Lett.* **106**, 217206 (2011).
- [99] T. Prosen and E. Ilievski, Families of quasilocal conservation laws and quantum spin transport, *Phys. Rev.*

- Lett. **111**, 057203 (2013).
- [100] E. Ilievski, M. Medenjak, T. Prosen, and L. Zadnik, Quasilocal charges in integrable lattice systems, *Journal of Statistical Mechanics: Theory and Experiment* **2016**, 064008 (2016).
 - [101] B. Bertini, F. Heidrich-Meisner, C. Karrasch, T. Prosen, R. Steinigeweg, and M. Žnidarič, Finite-temperature transport in one-dimensional quantum lattice models, *Rev. Mod. Phys.* **93**, 025003 (2021).
 - [102] X. Zotos, F. Naef, and P. Prelovsek, Transport and conservation laws, *Phys. Rev. B* **55**, 11029 (1997).
 - [103] E. Ilievski and T. Prosen, Thermodynamic bounds on drude weights in terms of almost-conserved quantities, *Communications in Mathematical Physics* **318**, 809–830 (2012).
 - [104] D. Ampelogiannis and B. Doyon, Almost everywhere ergodicity in quantum lattice models, *Communications in Mathematical Physics* **404**, 735–768 (2023).
 - [105] F. Weiner, P. Schmitteckert, S. Bera, and F. Evers, High-temperature spin dynamics in the heisenberg chain: Magnon propagation and emerging kardar-parisi-zhang scaling in the zero-magnetization limit, *Phys. Rev. B* **101**, 045115 (2020).
 - [106] M. Dupont and J. E. Moore, Universal spin dynamics in infinite-temperature one-dimensional quantum magnets, *Phys. Rev. B* **101**, 121106 (2020).
 - [107] J. De Nardis, S. Gopalakrishnan, and R. Vasseur, Nonlinear fluctuating hydrodynamics for kardar-parisi-zhang scaling in isotropic spin chains, *Phys. Rev. Lett.* **131**, 197102 (2023).
 - [108] B. Doyon, G. Perfetto, T. Sasamoto, and T. Yoshimura, Ballistic macroscopic fluctuation theory, *SciPost Phys.* **15**, 136 (2023).
 - [109] B. Bertini, P. Calabrese, M. Collura, K. Klobas, and C. Rylands, Nonequilibrium full counting statistics and symmetry-resolved entanglement from space-time duality, *Phys. Rev. Lett.* **131**, 140401 (2023).
 - [110] B. Doyon, G. Perfetto, T. Sasamoto, and T. Yoshimura, Emergence of hydrodynamic spatial long-range correlations in nonequilibrium many-body systems, *Phys. Rev. Lett.* **131**, 027101 (2023).
 - [111] V. B. Bulchandani, Kardar-parisi-zhang universality from soft gauge modes, *Phys. Rev. B* **101**, 041411 (2020).
 - [112] A. Bastianello, A. De Luca, B. Doyon, and J. De Nardis, Thermalization of a trapped one-dimensional bose gas via diffusion, *Phys. Rev. Lett.* **125**, 240604 (2020).
 - [113] E. I. Alvisi Bastianello, Žiga Krajnik, Landau-Lifschitz magnets: exact thermodynamics and transport (2024).

Supplementary Material

Landau-Lifschitz magnets: exact thermodynamics and transport

Alvise Bastianello, Žiga Krajnik, Enej Ilievski

This Supplementary Material covers the technical aspects, including the derivations, presented in the Letter. In particular:

1. In Section 1 we review the TBA description of the integrable quantum spin- S chains.
2. In Section 2 we provide the spin-waves limit analysis of the classical spin chain. This calculation is crucial to fix the proper normalization of the Lie-Poisson brackets that allows to identify the spin current with the usual GHD identities for the Drude weight.
3. In Section 3 we discuss in details the semiclassical limit of the TBA of the quantum spin chain.
4. In Section 4 we describe the numerical methods used in solving the TBA equations, and performing the microscopic simulations.

Notation for scalar products and convolutions in rapidity space. — In the main text, we introduced the short-hand notation for the scalar product $f_I \circ g_I \equiv \sum_I \int d\lambda f_I(\lambda) g_I(\lambda)$ for arbitrary functions f_I and g_I , where the summation over the modes I is replaced by an integral in the case of a continuous spectrum. Similarly, the convolution $T_{II'} \star f_{I'}$ is defined as $[T_{II'} \star f_{I'}](\lambda) \equiv \sum_{I'} \int d\lambda' T_{II'}(\lambda - \lambda') f_{I'}(\lambda')$.

1. THE INTEGRABLE QUANTUM SPIN- S CHAINS

In this Section, we provide a short summary of the excitation spectra and thermodynamics of the integrable quantum spin- S chains. We shall use these result as the starting point of our analysis In Section 3 where we systematically take the semiclassical limit of the quantum model and deduce the equations governing the classical thermodynamics of the Landau–Lifshitz spin chain.

The higher-spin analogue of the Heisenberg spin-1/2 chain can be obtained by employing the fusion technique [74, 75]. An infinite tower of local Hamiltonians can then be obtained in the usual fashion by taking the logarithmic derivatives of the fused commuting transfer matrix evaluated at a particular point. We shall not review the procedure here, since the spin- S Hamiltonians are given by rather cumbersome expressions, besides being inessential for the implementation of our program. Instead, the reader is referred to Refs. [77, 78] and references therein.

Thermodynamic Bethe Ansatz. — The exact thermodynamics of integrable models is describable within the Thermodynamic Bethe Ansatz (TBA) framework [73]. The general structure is as follows: the elementary excitations are magnons with bare momentum p . We use a convenient parametrization in terms of the rapidity variable $\lambda \in (-\Lambda, \Lambda)$. The cutoffs in the rapidity space Λ and the number of strings are model-dependent. Due to attractive interaction, magnons can bind into coherent bound states called Bethe strings. The internal quantum number of a string, $j \in \{1, 2, \dots, N\}$, is the binding number, i.e. the number of magnetization quanta – the $U(1)$ charge of a string. Each magnon excitation carries finite amount of (bare) charges. The total charge of an eigenstate is obtained by adding up the charges of individual magnons or strings. The bare energy, momentum and $U(1)$ charge (magnetization) are denoted by $e_j(\lambda)$, $p_j(\lambda)$ and m_j , respectively. In the thermodynamic limit, one describes macrostates with the so-called root density, which is interpreted as the phase-space density of these excitations and is denoted as $\rho_j(\lambda)$. In the thermodynamic limit, the total energy density, magnetization and more general conserved quantities can be expressed weighting the summation over the bare charges with the excitations' root density. For example, in an homogeneous system of size L one has

$$\lim_{L \rightarrow \infty} \frac{1}{L} \langle H \rangle = \sum_{j=1}^N \int_{-\Lambda}^{\Lambda} d\lambda e_j(\lambda) \rho_j(\lambda), \quad \lim_{L \rightarrow \infty} \frac{1}{L} \langle S^z \rangle = 1 - \sum_{j=1}^N \int d\lambda m_j \rho_j(\lambda) \quad (\text{S1})$$

Due to interactions, the allowed phase space for each excitation is renormalized by the presence of other quasiparticles. Hence, one introduces the total root density $\rho_j^t(\lambda)$ and the filling fraction $\vartheta_j(\lambda) = \rho_j(\lambda)/\rho_j^t(\lambda)$. The root density and total root densities are not independent, but are connected through the integral equation

$$\kappa_j \rho_j^t(\lambda) = \frac{\partial_\lambda p_j(\lambda)}{2\pi} - \sum_{j'} \int_{-\Lambda}^{\Lambda} d\lambda' T_{j,j'}(\lambda - \lambda') \rho_{j'}(\lambda'), \quad (\text{S2})$$

where $\kappa_j = \text{sign}(\partial_\lambda p_j)$ is the parity of the string and it is equal to the sign of $\partial_\lambda p_j(\lambda)$. $T_{j,j'}(\lambda)$ is the scattering kernel that accounts for interactions. Indeed, in the zero density limit $\rho_j \rightarrow 0$, and thus in the absence of scattering, the total root density becomes the bare one $|\partial_\lambda p_j|/(2\pi)$.

To obtain the root density that describes a thermal state, one needs to minimize the proper free energy. To this end, one introduces the Yang-Yang entropy

$$\mathcal{S} = L \sum_{j=1}^N \int_{-\Lambda}^{\Lambda} d\lambda \rho_j^t(\lambda) s(\vartheta_j(\lambda)), \quad (\text{S3})$$

where $s(x)$ is the entropy density. In quantum integrable models, the excitations have fermionic statistics and thus $s(x) = -x \log x - (1-x) \log(1-x)$. Thermodynamics is determined upon maximizing the entropy constrained to energy and magnetization conservation, reaching the equations [73]

$$\varepsilon_j(\lambda) = \beta e_j(\lambda) + \mu m_j + \sum_{j'=1}^N \int_{-\Lambda}^{\Lambda} d\lambda' T_{j,j'}(\lambda - \lambda') \kappa_{j'} \log(1 + e^{-\varepsilon_{j'}(\lambda')}). \quad (\text{S4})$$

Here the ‘effective energy’ ε_j was introduced to parametrize the filling fractions as $\vartheta_j(\lambda) = (e^{\varepsilon_j(\lambda)} + 1)^{-1}$. This set of equations, together with Eq. (S21), determines thermal states. The spin Drude weight can be exactly computed within the theory of Generalized Hydrodynamics [93] and reads

$$\mathcal{D} = \sum_{j=1}^N \int_{-\Lambda}^{\Lambda} d\lambda \rho_j(\lambda) (1 - \vartheta_j(\lambda)) (m_j^{\text{dr}} v_j^{\text{eff}}(\lambda))^2, \quad (\text{S5})$$

where $v_j^{\text{eff}}(\lambda)$ is the effective velocity of the quasiparticles renormalized by the background excitations, defined as $v_j^{\text{eff}}(\lambda) = (\partial_\lambda e_j(\lambda))^{\text{dr}} / (\partial_\lambda p_j(\lambda))^{\text{dr}}$ where for each test function $g_j(\lambda)$ the dressing operation $g_j(\lambda) \rightarrow g_j^{\text{dr}}(\lambda)$ is defined as

$$g_j^{\text{dr}}(\lambda) = g_j(\lambda) - \sum_{j'=1}^N \int_{-\Lambda}^{\Lambda} d\lambda' T_{j,j'}(\lambda - \lambda') \kappa_{j'} \vartheta_{j'}(\lambda') g_{j'}(\lambda'). \quad (\text{S6})$$

These general formulas need to be specified for the quantum magnet. In this case, one needs to distinguish the easy-axis regime $\varrho = \varrho_{\text{ea}} \in [0, +\infty)$ and the easy-plane regime $\varrho = i\varrho_{\text{ep}}$ with $\varrho_{\text{ep}} \in [0, \pi/(2S)]$. The isotropic point can be obtained as a limiting case of the easy-axis phase.

The easy-axis regime.— In this phase, the rapidity lives on a compact interval $\lambda \in [-\Lambda, \Lambda] = [-\pi/2, \pi/2]$, while the string’s index is unbounded $N = \infty$. One conveniently introduces the function

$$K_j(\lambda) = \frac{1}{2\pi i} \partial_\lambda \log \left(\frac{\sin(\lambda - i j \varrho_{\text{ea}}/2)}{\sin(\lambda + i j \varrho_{\text{ea}}/2)} \right). \quad (\text{S7})$$

Then the scattering kernel is computed as

$$T_{j,j'}(\lambda) = \sum_{a=1}^{\min(j-1,j')} K_{|j-j'|-1+2a}(\lambda) + \sum_{\ell=1}^{\min(j+1,j')} K_{|j-j'|-1+2a}(\lambda) \quad (\text{S8})$$

The bare momentum, energy and magnetization are

$$\frac{1}{2\pi} \partial_\lambda p_j(\lambda) = \sum_{a=1}^{\min(j,S)} K_{|j-j'|-1+2a}(\lambda), \quad e_j(\lambda) = 2 \sinh \varrho_{\text{ea}} \partial_\lambda p_j(\lambda) \quad m_j = 2j. \quad (\text{S9})$$

The parity is positive for all the strings $\kappa_j = 1$. In the easy-axis regime, there is an extra caveat concerning the magnetization. We are using the convention where excitations are placed on top of the all-spins-up reference state. By increasing the chemical potential, the magnetization covers the sector $[1, 0]$, but it cannot change sign. The other sector is described by using the \mathbb{Z}_2 symmetry of the model under a global flip in the magnetization sign: in this way, excitations are placed on top of the all-spins-up reference state, and cover the other magnetization sector. The same feature is well-known in the canonical spin-1/2 XXZ chain [53].

The easy-plane regime.— In the easy-plane, we parametrize the interaction as $\varrho = i\varrho_{\text{ep}}$. To guarantee the hermicity of the spin chain, interactions must be restricted to the region $\pi/\varrho_{\text{ep}} > 2S$. Similarly to the spin-1/2 XXZ chain, the strings' content greatly depends on the continued-fraction representation of π/ϱ_{ep} . For the sake of simplicity, and since this is sufficient for taking the semiclassical limit, we focus on the so called root of units $\varrho_{\text{ep}} = \pi/\ell$ with $\ell \in \mathbb{N}$. In the planar regime, the rapidity lives on the whole real axis $\Lambda = \infty$, while the number of strings is finite $j \in \{1, \dots, \ell\}$. The magnetization and parity are respectively

$$\begin{cases} m_j = 2j & j < \ell \\ m_\ell = 2 \end{cases} \quad \begin{cases} \kappa_j = 1 & j < \ell \\ \kappa_\ell = -1 \end{cases} \quad (\text{S10})$$

We define the auxiliary function

$$a_x^y = \frac{y}{\pi} \frac{\sin(\varrho_{\text{ep}} x)}{\cosh(2\lambda) - y \cos(\varrho_{\text{ep}} x)}. \quad (\text{S11})$$

Then, the scattering kernels can be written as

$$T_{j,k} = (1 - \delta_{m_j, m_k}) a_{|m_j - m_k|/2}^{\sigma_j \sigma_k}(\lambda) + a_{(m_j + m_k)/2}^{\sigma_j \sigma_k}(\lambda) + 2 \sum_{\ell=1}^{\min(m_j, m_k)/2-2} a_{|m_j - m_k|/2+2\ell}^{\sigma_j \sigma_k}. \quad (\text{S12})$$

The bare energy is $e_j(\lambda) = 2 \sin \varrho_{\text{ep}} \partial_\lambda p_j(\lambda)$, while the λ -derivative of the bare momentum is

$$p_j(\lambda) = 2\pi \sum_{k=1}^{\min(m_j, 2S)} a_{|m_j/2-2S|+2k-1}^{\sigma_j}(\lambda). \quad (\text{S13})$$

In the high-temperature limit, $\beta \rightarrow 0$, the TBA equations are rendered algebraic, depending only on the chemical potential μ . The occupation function, valid for any spin S , take the following explicit form [73]:

$$\vartheta_{j \leq \ell-2} = \frac{\sinh^2(\mu)}{\sinh^2(\mu(j+1))} \quad \vartheta_{\ell-1} = \frac{1}{1 + e^{\ell\mu} \frac{\sinh((\ell-1)\mu)}{\sinh(\mu)}} \quad \vartheta_\ell = \frac{1}{1 + e^{\ell\mu} \frac{\sinh(\mu)}{\sinh((\ell-1)\mu)}} \quad (\text{S14})$$

2. THE SPIN-WAVES LIMIT OF THE CLASSICAL SPIN CHAIN

In the limit of strong polarization $S_j^3 \sim 1$, the equation of motion can be linearized or, equivalently, the Hamiltonian can be expanded up to quadratic order in the fluctuations around the polarized state. In this limit, the excitations are spin-waves, i.e. non-interacting plane waves with Rayleigh-Jeans statistics whose thermodynamics can be easily computed. Since this limiting case is an important benchmark for our exact thermodynamic description, it is worth discussing the relevant details. We consider the lattice Hamiltonian in the easy-axis regime (2) and leave arbitrary the normalization of the Lie-Poisson brackets \mathcal{E} , i.e. $\{S^a, S^b\} = \mathcal{E} \epsilon_{abc} S^c$. By looking at the equation of motion $\frac{dS_j^a}{dt} = \mathcal{E} \epsilon_{abc} \frac{\partial H_{LLLL}}{\partial S_j^b} S_j^c$, and expanding up to linear order in S_j^1 and S_j^2 , we reach the approximated equation of motion

$$\frac{dS^+(k)}{dt} \simeq -i\omega_{\text{SW}}(k) S^+(k) \quad \omega_{\text{SW}}(k) = \mathcal{E} \frac{2\varrho_{\text{ea}}}{\sinh \varrho_{\text{ea}}} (\cosh \varrho_{\text{ea}} - \cos k) \quad (\text{S15})$$

where we define $S^\pm(k) = \sum_j e^{-ikj} \frac{1}{\sqrt{2}} (S_j^1 \pm iS_j^2)$. Importantly, the group velocity of the spin-waves is given by $v_{\text{SW}}(k) = \partial_k \omega_{\text{SW}}(k)$. One could be tempted to identify the frequency $\omega_{\text{SW}}(k)$ with the energy of the spin-waves $e_{\text{SW}}(k)$, but this is not the case: thermodynamic quantities, such as the expectation value of the Hamiltonian for example, are not \mathcal{E} -dependent, while $\omega_{\text{SW}}(k)$ is.

It turns out that the energy and the frequency differ for a simple \mathcal{E} -dependent proportionality factor $\omega_{\text{SW}}(k) = C(\mathcal{E})e_{\text{SW}}(k)$: the quickest way to fix $C(\mathcal{E})$ is looking at the Hamiltonian expectation value in the spin-waves limit. On the one hand, we use the thermodynamics of spin-waves: since they are non-interacting plane waves, their mode-density $n(k)$ follows Rayleigh-Jeans distribution $n(k) = 1/(\beta e_{\text{SW}}(k) + 2\mu)$, thus

$$\langle H_{\text{LLL}} \rangle \simeq \langle H_{\text{LLL}} \rangle_{\text{vac}} + L \int \frac{dk}{2\pi} \frac{e_{\text{SW}}(k)}{\beta e_{\text{SW}}(k) + 2\mu} \quad (\text{S16})$$

where $\langle H_{\text{LLL}} \rangle_{\text{vac}}$ is the expectation value of the Hamiltonian on the fully polarized state. In particular, on infinite temperature states $\beta = 0$ we find $\langle H_{\text{LLL}} \rangle \simeq \langle H_{\text{LLL}} \rangle_{\text{vac}} + L \frac{\mathcal{E}}{C(\mathcal{E})} \frac{\varrho_{\text{ea}} \coth \varrho_{\text{ea}}}{\mu}$. On the other hand, we can expand the Hamiltonian for small fluctuations around the polarized state

$$H_{\text{LLL}} \simeq \langle H_{\text{LLL}} \rangle_{\text{vac}} + \sum_j \frac{2\varrho_{\text{ea}}}{\sinh \varrho_{\text{ea}}} \left(\frac{\cos \varrho_{\text{ea}}}{4} (S_j^1 S_j^1 + S_j^2 S_j^2 + S_{j+1}^1 S_{j+1}^1 + S_{j+1}^2 S_{j+1}^2) - \frac{1}{2} (S_j^1 S_{j+1}^1 + S_j^2 S_{j+1}^2) \right). \quad (\text{S17})$$

On infinite temperature states, spins at different positions are uncorrelated, thus $\langle S_j^a S_{j+1}^b \rangle = \langle S_j^a \rangle \langle S_{j+1}^b \rangle$, while for large μ one readily computes $\langle S_j^1 S_j^1 + S_j^2 S_j^2 \rangle \simeq \frac{2}{\mu}$, thus finding $H_{\text{LLL}} \simeq \langle H_{\text{LLL}} \rangle_{\text{vac}} + L \frac{2\varrho_{\text{ea}} \coth \varrho_{\text{ea}}}{\mu}$: imposing the consistency with the spin-waves thermodynamics, we therefore fix $C(R) = \frac{\mathcal{E}}{2}$ and thus

$$e_{\text{SW}}(k) = \frac{4\varrho_{\text{ea}}}{\sinh \varrho_{\text{ea}}} (\cosh \varrho_{\text{ea}} - \cos k). \quad (\text{S18})$$

Notice that only in the case where $\mathcal{E} = 2$, the spin-waves group velocity is the momentum derivative of the energy $v_{\text{SW}}(k) = \partial_k e_{\text{SW}}(k)$, which is the canonical convention in GHD. We notice the spin-waves analysis of the easy-plane is readily obtained by analytical continuation.

3. THE SEMICLASSICAL LIMIT OF THE QUANTUM TBA

In this section, we provide the details of the semiclassical limit of the TBA of the integrable quantum magnet, summarized in Section (1). We performed the semiclassical limit at the level of TBA. To make sure the limit yields the lattice Hamiltonian given by Eq. (2) (with the Lie-Poisson bracket normalization $\mathcal{E} = 2$), we have performed several consistency checks. In particular, (i) the spin wave limit is analytically retrieved, (ii) at the isotropic point we agree with Ref. [80], (iii) in the continuum limit, the dispersion relations and scattering kernels match the well-known expression for the Landau-Lifschitz field theory, (iv) the large-spin limit of the fundamental commutation (RLL) relation yields the (quadratic) Sklyanin algebra associated with the axially anisotropic lattice Landau-Lifshitz model (not reported), and finally (v) our analytics complies with great accuracy with ab initio numerical simulations.

As we discussed in the main text, the semiclassical limit is achieved by combining a large spin limit $S \rightarrow \infty$ with a small interaction limit. For the sake of clarity, we analyze separately the easy-axis and easy-plane regimes. We report the equations for the isotropic point and finally discuss the continuum limit. Within this section, we add a label “q” to quantities belonging to the quantum model.

1. The easy-axis regime

We use the quantum spin S as a control parameter and rescale the quantum interaction as $\varrho_{\text{ea}} = (2S)\varrho_{\text{ea};q}$: we will check that this rescaling gives the correct interaction in the classical model by looking at the spin-waves limit. The semiclassical limit of the easy-axis regime closely follows the analysis of the attractive Non-Linear Schrödinger [84] and sine-Gordon model [85]. Further details can be found in these references, here we focus on the main points. Finite TBA equations are obtained by assuming the strings can be replaced by a continuous spectral parameter σ with the correspondence $2S\sigma \leftrightarrow j$. Using this definition, in the large S limit one obtains

$$T_{q;j,j'}(\lambda) \rightarrow 2ST_{\sigma,\sigma'}(\lambda), \quad T_{\sigma,\sigma'}(\lambda) = \frac{1}{\pi\varrho_{\text{ea}}} \log \left(\frac{\cosh((\sigma + \sigma')\varrho_{\text{ea}}) - \cos(2\lambda)}{\cosh((\sigma - \sigma')\varrho_{\text{ea}}) - \cos(2\lambda)} \right). \quad (\text{S19})$$

Notice the useful identity $\int_{-\pi/2}^{\pi/2} d\lambda T_{\sigma,\sigma'}(\lambda) = 2\min(\sigma, \sigma')$. The root density of each quantum string vanishes as $\rho_{q;j} \rightarrow \frac{1}{2S}\rho_{\sigma}(\lambda)$: the system accommodates for the growing magnetization by populating more strings. In contrast,

the quantum total root density diverges $\rho_{q;j}^t(\lambda) \rightarrow 2S\rho_\sigma^t(\lambda)$. Indeed, the bare momentum and magnetization diverge as $\partial_\lambda p_{q;j} \rightarrow 2S\partial_\lambda p_\sigma(\lambda)$ and $m_{q;j} \rightarrow 2Sm_\sigma$, while the energy has a finite limit $e_{q;j} \rightarrow e_\sigma(\lambda)$ and the parity is positive for all modes $\kappa_\sigma = 1$. We define $\partial_\lambda p_\sigma(\lambda) = \pi T_{\sigma,1}(\lambda)$, $e_\sigma(\lambda) = 2\varrho_{\text{ea}}\partial_\lambda p_\sigma(\lambda)$ and $m_\sigma = 2\sigma$. We finally look at the limit of the quantum Yang-Yang entropy: here, extra caveat should be taken due to apparently divergent terms

$$\mathcal{S}_q \rightarrow L \int_{\delta_S}^{\infty} d\sigma \int_{-\pi/2}^{\pi/2} d\lambda [\rho_\sigma(\lambda) - \rho_\sigma(\lambda) \log(\vartheta_\sigma(\lambda)) + 2 \log(2S)\rho_\sigma(\lambda)]. \quad (\text{S20})$$

Above, we introduced the classical filling $\vartheta_\sigma(\lambda) = \rho_\sigma(\lambda)/\rho_\sigma^t(\lambda)$. In the integrand, a logarithmic divergent term appears: this must be compensated by another divergent counterterm that arises from small strings. For this reason, we introduce a cutoff $\delta_S \rightarrow 0$: its value must be fixed in a self-consistent manner, by requiring the final TBA equations obtained by minimizing the free energy are finite. Only after this, the limit $S \rightarrow \infty$ is safely taken. This procedure has been introduced in Refs. [84, 85]: following the same steps, one needs to impose $\log(2S\delta_S) = 1$ and finally taking the $S \rightarrow \infty$ limit one reaches the set of TBA equations

$$\sigma^2 \varepsilon_\sigma(\lambda) = \beta e_\sigma(\lambda) + \mu m_\sigma + \int_0^\infty d\sigma' d\lambda' T_{\sigma,\sigma'}(\lambda - \lambda') \frac{e^{-(\sigma')^2 \varepsilon_{\sigma'}(\lambda')} - 1}{(\sigma')^2}. \quad (\text{S21})$$

where the effective energy ε_σ parametrizes the filling function as $\vartheta_\sigma(\lambda) = \sigma^{-2} e^{-\sigma^2 \varepsilon_\sigma(\lambda)}$. At small values of σ , ε_σ reaches a finite value, hence the filling function develops a $\sim 1/\sigma^2$ divergence. As in the quantum XXZ chain [53], there are two disconnected sets of TBA equations corresponding to a two-fold degeneracy of the vacuum state, requiring and extra \mathbb{Z}_2 label for specifying the corresponding sector of positive or negative density of magnetization.

The semiclassical limit straightforwardly extends to the definition of the dressing operation $g_\sigma(\lambda) \rightarrow g_\sigma^{\text{dr}}(\lambda)$ as

$$g_\sigma^{\text{dr}}(\lambda) = g_\sigma(\lambda) - \int_0^\infty d\lambda' T_{\sigma,\sigma'}(\lambda - \lambda') \vartheta_{\sigma'}(\lambda') g_{\sigma'}^{\text{dr}}(\lambda'), \quad (\text{S22})$$

and to the spin Drude weight

$$\mathcal{D} = \int_0^\infty d\sigma \int_{-\pi/2}^{\pi/2} d\lambda \rho_\sigma(\lambda) [m_\sigma^{\text{dr}}(\lambda) v_\sigma^{\text{eff}}(\lambda)]^2, \quad (\text{S23})$$

with $v_\sigma^{\text{eff}}(\lambda) = (\partial_\lambda e_\sigma)^{\text{dr}}/(\partial_\lambda p_\sigma)^{\text{dr}}$. At large temperatures, the Drude weight diverges due to the singular dressed velocity $\lim_{(\sigma,\lambda) \rightarrow (1,0)} |v_\sigma^{\text{eff}}(\lambda)| = +\infty$ inherited by the singularities of the bare energy and momentum. To extract the singularity, we proceed as follows. We first change variable from the rapidity to energy E by imposing $E = e_\sigma(\lambda)$: integrals will be carried out in the space (σ, E) . Being mostly interested in thermal states, we use the fact that the integrand in the Drude weight is symmetric $\lambda \rightarrow -\lambda$, hence focus on positive λ . The singularity at $(\sigma, \lambda) = (1, 0)$ is mapped into $E \rightarrow \infty$, hence we split the Drude weight in two contributions

$$\mathcal{D} = \text{finite part} + 2 \int_0^\infty d\sigma \int_{E_c}^\infty \frac{dE}{2\pi} \left[\vartheta_\sigma(\lambda) \frac{(\partial_\lambda p_\sigma)^{\text{dr}}}{\partial_\lambda e_\sigma} [m_\sigma^{\text{dr}}(\lambda) v_\sigma^{\text{eff}}(\lambda)]^2 \right]_{E=e_\sigma(\lambda)} \quad (\text{S24})$$

Above, E_c is some large, but otherwise arbitrary, cutoff. At large E , we can extract from the effective energy $\varepsilon_\sigma(\lambda)$ its singular part, by defining $\varepsilon_{\text{NS}} = \lim_{(\sigma,\lambda) \rightarrow (1,0)} (\varepsilon_\sigma(\lambda) - \beta \sigma^{-2} e_\sigma)$, which is finite. Furthermore, the divergence in the effective velocity is due to the bare energy and momentum, hence we can approximate $v_\sigma^{\text{eff}}(\lambda) \rightarrow (\partial_\lambda e_\sigma)/(\partial_\lambda p_\sigma)$. In the same spirit, we expand the energy $e_\sigma(\lambda)$ around the singularity and obtain the approximate change of variables $\frac{1}{2}(2\lambda)^2 + \frac{1}{2}\varrho_{\text{ea}}^2(1-\sigma)^2 \simeq e^{-E/2}(\cosh(2\varrho_{\text{ea}}) - 1)$. Plugging these approximations in Eq. (S24) and taking the integral over σ , at the leading order we obtain

$$\mathcal{D} = \text{finite part} + \frac{1}{2} (m_1^{\text{dr}}(0))^2 e^{-\varepsilon_{\text{NS}}} \int_{E_c}^\infty dE \frac{e^{-\beta E}}{E}. \quad (\text{S25})$$

The last integral has a logarithmic singularity $\sim -\log \beta$, showing the divergence of the Drude weight in the infinite temperature limit. In Fig. S1, we benchmark the TBA equations by computing the expectation value of the magnetization and energy on thermal states and comparing with ab-initio Monte Carlo simulations, finding excellent agreement.

The infinite-temperature limit.— It is worth focusing on the infinite temperature limit by sending $\beta \rightarrow 0$ in Eq. (S21). The integral equation now becomes translational invariant in the rapidity space, therefore the effective energy

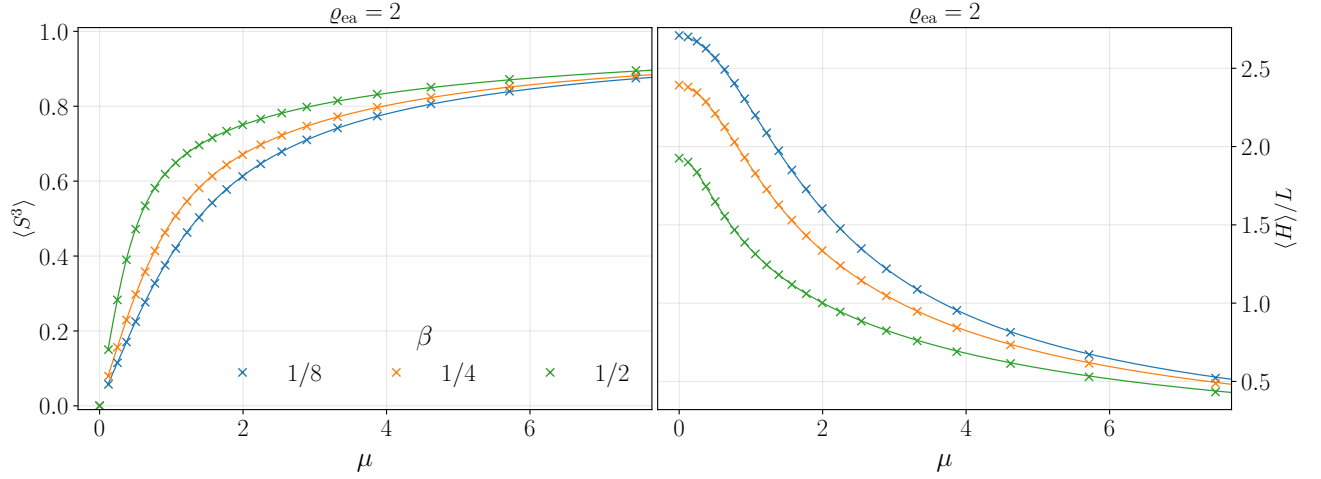


FIG. S1. Average magnetization (left) and energy (right) obtained by solving classical TBA equations (solid lines) compared with Monte-Carlo simulation (crosses) in the easy-axis regime with $\rho_{\text{ea}} = 2$ for $\beta \in \{1/8, 1/4, 1/2\}$. Monte Carlo error bars are negligible on the plot's scale and thus omitted.

becomes constant in the rapidity space $\varepsilon_\sigma(\lambda) \rightarrow \varepsilon_\sigma$. By averaging over λ , we can integrate the scattering kernel using its normalization, and eventually reaching the simplified equations

$$\sigma^2 \varepsilon_\sigma = 2\mu\sigma + \int_0^\infty d\sigma' 2 \min(\sigma, \sigma') \frac{e^{-(\sigma')^2 \varepsilon_{\sigma'}} - 1}{(\sigma')^2}. \quad (\text{S26})$$

This integral equation is formally identical to that faced in extracting the low-temperature behavior of the sine-Gordon field theory [85] and can be analytically solved: we leave to the quoted reference a more detailed discussion, here we report the final result, yielding $e^{-\sigma^2 \varepsilon_\sigma} = \frac{(\mu\sigma)^2}{\sinh^2(\mu\sigma)}$. The exact filling fraction can be used in the dressing equations (S22). Let us assume that the test function $g_\sigma(\lambda)$ has the the following properties: *i*) it is constant over the rapidities and *ii*) it is linear in σ , i.e. $g_\sigma(\lambda) = \bar{g}\sigma$. Then, the dressing equation can be analytically solved $g_\sigma^{\text{dr}} = \bar{g}u(2\mu\sigma)/(2\mu)$ with $u(x) = x \coth(x/2) - 2$ [85].

These assumptions are verified by the bare magnetization, hence the dressed magnetization m_σ^{dr} can be computed exactly on infinite temperature thermal states. One can finally compute the total magnetization as

$$\langle S^z \rangle = 1 - \int_{-\pi/2}^{\pi/2} d\lambda \int_0^\infty d\sigma m_\sigma \rho_\sigma(\lambda) = 1 - \int_{-\pi/2}^{\pi/2} \frac{d\lambda}{2\pi} \int_0^\infty d\sigma m_\sigma \vartheta_\sigma(\lambda) (\partial_\lambda p_\sigma)^{\text{dr}} = 1 - \int_{-\pi/2}^{\pi/2} \frac{d\lambda}{2\pi} \int_0^\infty d\sigma m_\sigma^{\text{dr}} \vartheta_\sigma(\lambda) (\partial_\lambda p_\sigma). \quad (\text{S27})$$

Since the dressed magnetization and the filling fraction on infinite-temperature states are rapidity-independent, the integral over $\partial_\lambda p_\sigma$ can be factorized $\int d\lambda \frac{\partial_\lambda p_\sigma}{2\pi} = \min(\sigma, 1)$. The last integral over σ can be easily computed, giving $\langle S^z \rangle = -\frac{1}{\mu} + \coth \mu$ which matches with the ab initio computation from the microscopic model. In the last passage Eq. (S27), we use the symmetry $\int_{-\pi/2}^{\pi/2} d\lambda \int_0^\infty d\sigma \vartheta_\sigma(\lambda) g_\sigma^{\text{dr}}(\lambda) h_\sigma(\lambda) = \int_{-\pi/2}^{\pi/2} d\lambda \int_0^\infty d\sigma \vartheta_\sigma(\lambda) g_\sigma(\lambda) h_\sigma^{\text{dr}}(\lambda)$ that holds for any test function $g_\sigma(\lambda)$ and $h_\sigma(\lambda)$.

The classical entropy.— It is expected that the limit of the quantum entropy (S20) should describe the classical entropy, but dealing with the apparent $\log S$ divergences seems challenging. Therefore, we use another route: we postulate the entropy can be written as $\mathcal{S} = L \int d\sigma \int d\lambda \rho_\sigma^t s_\sigma(\vartheta_\sigma) + LC$ with a proper entropy weight s_σ and possibly a constant C . Then, we consistently require that the minimization of the free energy $F = \beta \langle H \rangle + \mu \langle M^3 - M_{\text{vac}}^3 \rangle - \mathcal{S}$ gives Eq. (S21). After straightforward manipulations, we obtain $s_\sigma(\vartheta_\sigma) = \vartheta_\sigma - 1/\sigma^2 - \log(\sigma^2 \vartheta_\sigma) \vartheta_\sigma$. To fix the constant C , we compute the free energy $F = L \int_0^\infty d\sigma \int d\lambda \frac{\partial_\lambda p_\sigma}{2\pi} \mathcal{F}_\sigma(\vartheta_\sigma) - LC$ with $\mathcal{F}_\sigma(\vartheta_\sigma) = \vartheta_\sigma s'_\sigma(\vartheta_\sigma) - s_\sigma(\vartheta_\sigma) = \frac{1}{\sigma^2} - \vartheta_\sigma(\lambda)$: using that for $\beta = 0$ the filling is independent over λ , we carry out the rapidity integral over $\partial_\lambda p_\sigma$ hence we obtain

$$F = L \int_0^\infty d\sigma \frac{\min(\sigma, 1)}{\sigma^2} \left(1 - \frac{(\mu\sigma)^2}{\sinh^2(\mu\sigma)} \right) - LC = L(\mu + \log(\mu/\sinh \mu) - C). \quad (\text{S28})$$

On the other hand, the partition function of a classical spin in a magnetic field and with flat measure on the unit sphere is $Z = \frac{1}{4\pi} \int_0^\pi d\phi \int_0^{2\pi} d\theta \sin \phi e^{\mu \cos \phi - \mu} = e^{-\mu} \frac{\sinh \mu}{\mu}$, hence $F = -L \log Z$ and finally, by comparison, $C = 0$.

The spin-waves limit.— We now focus on the strongly polarized limit $\mu \gg 1$, and retrieve from the exact TBA the spin-waves thermodynamics outlined in Section 2. spin-waves are radiative in nature and should be recovered by the solitonic TBA: we closely follow the same procedure used in studying the low-temperature limit of the sine-Gordon field theory [85].

In the limit $\mu \gg 1$, only solitons with small σ are populated. In this limit, the kernel $T_{\sigma,\sigma'}(\lambda)$ is increasingly peaked at small rapidities and can be eventually approximated with a delta function $T_{\sigma,\sigma'}(\lambda) \simeq 2 \min(\sigma, \sigma') \delta(\lambda)$ for $\sigma \ll 1$ and $\sigma' \ll 1$. By plugging this approximation in Eq. (S21) and furthermore approximating $e_\sigma(\lambda) \simeq \sigma e^{(1)}(\lambda)$, with $e^{(1)}(\lambda) = \lim_{\sigma \rightarrow 0} \sigma^{-1} e_\sigma(\lambda)$, one obtains

$$\sigma^2 \varepsilon_\sigma(\lambda) = \beta e^{(1)}(\lambda) + 2\mu\sigma + \int_0^\infty d\sigma' 2 \min(\sigma, \sigma') \frac{e^{-(\sigma')^2 \varepsilon_{\sigma'}(\lambda)} - 1}{(\sigma')^2}. \quad (\text{S29})$$

This equation is formally identical to Eq.(S26), with a parametric dependence on the rapidity, hence it can be solved as before. The same strategy can be used for the dressing equations. To recover radiation, it is instructive looking at the expectation value of a charge $q_\sigma(\lambda)$ on a low temperature state. In particular, we fix the rapidity and look at the cumulative effects of solitons (see Ref. [85] for details)

$$\int_0^\infty d\sigma \rho_\sigma q_\sigma(\lambda) \simeq \frac{1}{2\pi} \frac{\partial_\lambda p^{(1)}(\lambda)}{\beta e^{(1)}(\lambda) + \mu} q^{(1)}(\lambda). \quad (\text{S30})$$

The r.h.s. contribution is formally identical to the thermal contribution of a radiative mode, hence obeying the Rayleigh-Jeans distribution, with energy $e^{(1)}(\lambda)$, momentum derivative $\partial_\lambda p^{(1)}(\lambda) = \lim_{\sigma \rightarrow 0} \sigma^{-1} \partial_\lambda p_\sigma(\lambda)$ and carrying a charge $q^{(1)}(\lambda) = \lim_{\sigma \rightarrow 0} \sigma^{-1} q_\sigma(\lambda)$. To push further this identification, we define the momentum $k \rightarrow k(\lambda) = \int^\lambda d\lambda' \partial_{\lambda'} p^{(1)}(\lambda') = 2 \arctan(\tan \lambda \coth(\varrho_{\text{ea}}/2)) + \pi$. By inverting this relation $\lambda(k)$ and plugging in the energy $e^{(1)}(\lambda)$, we obtain the energy of spin waves $e_{\text{SW}}(k) = e^{(1)}(\lambda(k)) = \frac{4\varrho_{\text{ea}}}{\sinh \varrho_{\text{ea}}} (\cosh \varrho_{\text{ea}} - \cos k)$ and thus we match the approximate thermodynamics of small fluctuations nearby the ferromagnetic vacuum discussed in Section 2. Notice that, furthermore, in the spin wave limit we readily find that $v_\sigma^{\text{eff}}(\lambda) \rightarrow \partial_k e_{\text{SW}}(k)$, thus fixing to $R = 2$ the normalization in the Lie-Poisson brackets, according to the argument presented in Section 2.

2. The easy-plane regime

We now discuss in detail the semiclassical limit of the easy-plane regime. As in the previous case, we rescale the interaction as $\varrho_{\text{ep}} = (2S)\varrho_{\text{ep};q}$ and take the limit $S \rightarrow \infty$. As discussed in Section 1, the TBA of the quantum chain depends on the interactions in a seemingly non-continuous way. However, this structure is washed away in the semiclassical limit, therefore for the sake of simplicity we can consider the so called roots of unity $\varrho_{\text{ep};q} = \pi/\ell_q$ with ℓ_q a large integer. For convenience, we define $\ell = \ell_q/(2S)$: notice ℓ remains constant in the semiclassical limit. In the quantum chain there are ℓ_q strings which behave differently in order to achieve a finite semiclassical limit: the strings $j \in \{1, \dots, \ell_q - 2\}$ behave alike the easy-axis case and can be well-described by solitons with a continuum spectral parameter $\sigma \in [0, \ell]$, with the correspondence $\sigma = j/(2S)$. For these modes, we borrow the same notation as the easy-axis regime. The two last strings behave differently: the last string contributes as a radiative mode denoted with “R”, and its scaling is similar to semiclassical limits of field theories with only radiation [82]. In contrast, the second last describes solitons with no bare energy or momentum, but maximum magnetization, and we conventionally denote them with “Z”. In short, the filling functions and root densities scale as

$$\vartheta_{q;j < \ell_q - 1}(\lambda) \rightarrow \frac{1}{(2S)^2} \vartheta_\sigma(\lambda), \quad \vartheta_{q;\ell_q - 1}(\lambda) \rightarrow \frac{1}{2S} \vartheta_Z(\lambda), \quad \vartheta_{q;\ell_q}(\lambda) = 1 - \frac{1}{2S} \vartheta_R^{-1}(\lambda). \quad (\text{S31})$$

$$\rho_{q;j < \ell_q - 1}(\lambda) \rightarrow \frac{1}{2S} \rho_\sigma(\lambda), \quad \rho_{q;\ell_q - 1}(\lambda) \rightarrow \rho_Z(\lambda), \quad \rho_{q;\ell_q}(\lambda) = 2S \rho_R(\lambda). \quad (\text{S32})$$

while the quantum kernels behave as

$$T_{q;j < \ell_q - 1, j' < \ell_q - 1}(\lambda) \rightarrow 2ST_{\sigma,\sigma'}(\lambda), \quad T_{q;j < \ell_q - 1, \ell_q}(\lambda) \rightarrow T_{\sigma,R}(\lambda), \quad (\text{S33})$$

$$T_{q;\ell_q - 1, \ell_q}(\lambda) \rightarrow T_{Z,R}, \quad T_{q;\ell_q, \ell_q}(\lambda) \rightarrow \delta(\lambda) + \frac{1}{2S} T_{R,R}(\lambda), \quad (\text{S34})$$

with

$$T_{\sigma,\sigma'}(\lambda) = \frac{1}{\varrho_{\text{ep}}\pi} \log \left[\frac{\cosh(2\lambda) - \cos(\varrho_{\text{ep}}(\sigma + \sigma'))}{\cosh(2\lambda) - \cos(\varrho_{\text{ep}}(\sigma - \sigma'))} \right], \quad T_{\sigma,\text{R}}(\lambda) = T_{\text{R},\sigma}(\lambda) = -\frac{2}{\pi} \frac{\sin(\varrho_{\text{ep}}\sigma)}{\cosh(2\lambda) + \cos(\varrho_{\text{ep}}\sigma)}, \quad (\text{S35})$$

$$T_{\text{R},\text{R}}(\lambda) = -\frac{\varrho_{\text{ep}}}{2\pi} \partial_\lambda \mathcal{P} \coth(\lambda), \quad T_{\text{Z},\text{R}}(\lambda) = T_{\text{R},\text{Z}}(\lambda) = -\delta(\lambda). \quad (\text{S36})$$

Omitted classical kernels vanish in the limit. The self-interaction of radiation $T_{\text{R},\text{R}}$ needs further explanation: the double pole must be regularized within the principal value regularization, denoted with \mathcal{P} such as

$$\int_{-\infty}^{\infty} d\lambda' T_{\text{R},\text{R}}(\lambda - \lambda') g_{\text{R}}(\lambda') = \left[\frac{\varrho_{\text{ep}}}{2\pi} \coth[2(\lambda' - \lambda)] g_{\text{R}}(\lambda') \right]_{\lambda'=-\infty}^{\lambda=\infty} + \lim_{\epsilon \rightarrow 0^+} \int_{\lambda' \in [\infty, -\epsilon] \cup [\epsilon, +\infty]} d\lambda' \frac{\varrho_{\text{ep}}}{2\pi} \coth[2(\lambda - \lambda')] \partial_{\lambda'} g_{\text{R}}(\lambda'), \quad (\text{S37})$$

for any test function $g_{\text{R}}(\lambda)$. It is worth noticing the normalizations

$$\int d\lambda T_{\sigma,\sigma}(\lambda) = 2 \min(\sigma, \sigma') - 2\sigma\sigma'/\ell, \quad \int d\lambda T_{\sigma,\text{R}}(\lambda) = -2\sigma/\ell, \quad \int d\lambda T_{\text{R},\text{R}}(\lambda) = -2/\ell. \quad (\text{S38})$$

Verifying that this scaling gives finite dressing equations in the $S \rightarrow \infty$ limit is a lengthy, but straightforward, derivation. When computing the semiclassical limit of the Yang-Yang entropy, divergent terms akin to the easy-axis regime are obtained

$$\mathcal{S}_q \rightarrow L \int_{-\infty}^{\infty} d\lambda' \left\{ \int_{\delta_S}^{\ell} d\sigma \rho_\sigma (1 - \log \vartheta_\sigma) + \rho_{\text{R}}^t (\log \vartheta_{\text{R}} + 1) + \rho_{\text{Z}} (1 - \log \vartheta_{\text{Z}}) + \log(2S) \left[\rho_{\text{Z}}^t + \rho_{\text{Z}} + \int_{\delta_S}^{\ell} d\sigma 2\rho_\sigma \right] \right\}. \quad (\text{S39})$$

The explicit $\log(2S)$ divergence is counterbalanced by a divergence at small σ regularized by δ_S : finite TBA equations can be obtained if one imposes again $\log(2S\delta_S) = 1$, leading to

$$\sigma^2 \varepsilon_\sigma(\lambda) = \beta \sigma e_\sigma(\lambda) + \mu m_\sigma - \frac{2\sigma}{\ell} \log \ell + \int_0^\ell d\sigma' \int d\lambda T_{\sigma,\sigma'}(\lambda - \lambda') \frac{e^{-(\sigma')^2 \varepsilon_{\sigma'}(\lambda')} - 1}{(\sigma')^2} + \int d\lambda T_{\sigma,\text{R}}(\lambda - \lambda') \log \varepsilon_{\text{R}}(\lambda'), \quad (\text{S40})$$

$$\varepsilon_{\text{R}}(\lambda) = \beta e_{\text{R}}(\lambda) + \mu m_{\text{R}} + \frac{2}{\ell} - \frac{2}{\ell} \log \ell + \int_0^\ell d\sigma' \int d\lambda T_{\text{R},\sigma'}(\lambda - \lambda') \frac{e^{-(\sigma')^2 \varepsilon_{\sigma'}(\lambda')} - 1}{(\sigma')^2} + \int d\lambda T_{\text{R},\text{R}}(\lambda - \lambda') \log \varepsilon_{\text{R}}(\lambda') + \int d\lambda T_{\text{R},\text{Z}}(\lambda - \lambda') e^{-\varepsilon_{\text{Z}}(\lambda')}, \quad (\text{S41})$$

$$\varepsilon_{\text{Z}}(\lambda) = \mu m_{\text{Z}} + \int d\lambda T_{\text{R},\text{Z}}(\lambda - \lambda') \log \varepsilon_{\text{R}}(\lambda'). \quad (\text{S42})$$

The bare magnetizations are respectively $m_\sigma = 2\sigma$, $m_{\text{Z}} = 2\ell$, $m_{\text{R}} = 2$, while the bare energies are $e_\sigma = 2\varrho_{\text{ep}}\partial_\lambda p_\sigma$, $e_{\text{R}} = 2\varrho_{\text{ep}}\partial_\lambda p_{\text{R}}$ and $e_{\text{Z}} = 2\varrho_{\text{ep}}\partial_\lambda p_{\text{Z}}$, where

$$\partial_\lambda p_\sigma(\lambda) = \pi T_{\sigma,1}(\lambda), \quad \partial_\lambda p_{\text{R}} = -\frac{2 \sin \varrho_{\text{ep}}}{\cosh(2\lambda) + \cos \varrho_{\text{ep}}}, \quad \partial_\lambda p_{\text{Z}} = 0. \quad (\text{S43})$$

The classical modes inherit the parity of the quantum ones, so $\kappa_\sigma = 1$, $\kappa_{\text{Z}} = 1$ and $\kappa_{\text{R}} = -1$. Above, the effective energies parametrize the filling functions as

$$\vartheta_\sigma(\lambda) = \frac{e^{-\sigma^2 \varepsilon_\sigma(\lambda)}}{\sigma^2}, \quad \vartheta_{\text{R}}(\lambda) = \frac{1}{\varepsilon_{\text{R}}(\lambda)}, \quad \vartheta_{\text{Z}}(\lambda) = e^{-\varepsilon_{\text{Z}}(\lambda)}. \quad (\text{S44})$$

Unlike in the easy-axis regime a single set of TBA equations suffices to capture states from both magnetization sectors by tuning the chemical $\mu \in \mathbb{R}$.

The dressing operation has the canonical form where the sum over all the particle species should be taken into account, weighted with the proper scattering kernels. Finally, we focus on the Drude weight: by taking the semiclassical limit of the quantum expression, one readily reaches

$$\mathcal{D} = \int d\lambda \int_0^\ell d\sigma \rho_\sigma(\lambda) (m_\sigma^{\text{dr}}(\lambda) v_\sigma^{\text{eff}}(\lambda))^2 + \rho_{\text{Z}}(\lambda) (m_{\text{Z}}^{\text{dr}}(\lambda) v_{\text{Z}}^{\text{eff}}(\lambda))^2 + \rho_{\text{R}}(\lambda) \vartheta_{\text{R}}(\lambda) (m_{\text{R}}^{\text{dr}}(\lambda) v_{\text{R}}^{\text{eff}}(\lambda))^2. \quad (\text{S45})$$

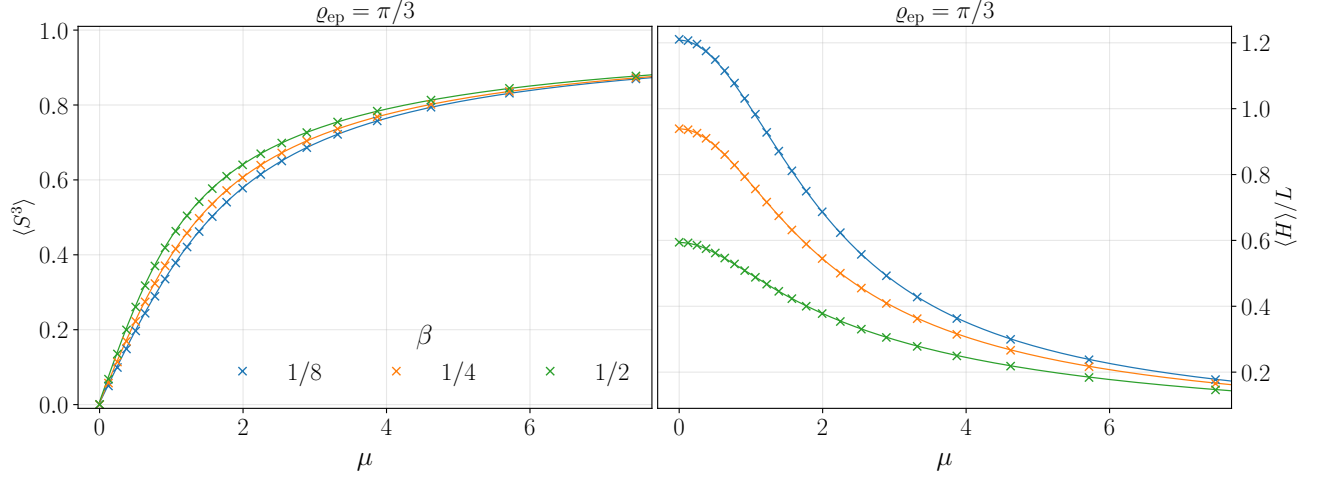


FIG. S2. Average magnetization (left) and energy (right) obtained by solving classical TBA equations (solid lines) compared with Monte-Carlo simulation (crosses) in the easy-plane regime with $\rho_{\text{ea}} = \pi/3$ for $\beta \in \{1/8, 1/4, 1/2\}$. Monte Carlo error bars are negligible on the plot's scale and thus omitted.

Similarly to the easy-axis case, the singularity of the bare energy placed at $(\sigma, \lambda) = (1, 0)$ manifest as a singularity of the Drude weight at zero temperature $\sim -\log \beta$: the derivation of the divergence follow the same analysis of the easy-axis, and it is thus omitted. In Fig. S2, we benchmark our TBA equations on the average magnetization and energy, with good agreement.

The infinite-temperature limit.— As in the axial regime, also in the planar case the filling function becomes rapidly independent in the infinite temperature limit $\beta \rightarrow 0$. The infinite-temperature TBA equations are easily written, but they are not easy to solve. We managed to find a solution by taking the semiclassical limit of the known solution for the quantum chain (S14) and check a posteriori its correctness, obtaining

$$\vartheta_\sigma = \frac{\mu^2}{\sinh^2(\mu\sigma)}, \quad \vartheta_R = e^{-\ell\mu} \frac{\sinh(\ell\mu)}{\mu}, \quad \vartheta_Z = e^{-\mu\ell} \frac{\mu}{\sinh(\ell\mu)}. \quad (\text{S46})$$

To compute the total magnetization we follow another route compared with the easy-axis regime passing through the free-energy: the discussion is postpone to the next paragraph.

The classical entropy.— To compute the classical entropy, we pursue the same strategy we used in the easy-axis regime: we postulate the entropy has the form $\mathcal{S} = L \int d\lambda [\int d\sigma \rho_\sigma^t s_\sigma(\vartheta_\sigma) + \rho_R^t s_R(\vartheta_R) + s_Z(\vartheta_Z)] + LC$ with C a constant, and impose that the TBA equations (S40)(S41)(S42) are recovered by minimizing the free energy.

This simple analysis gives

$$s_\sigma(\vartheta_\sigma) = \vartheta_\sigma - 1/\sigma^2 - \log(\sigma^2 \vartheta_\sigma) \vartheta_\sigma, \quad s_R(\vartheta_R) = 1 - \log(\ell/\vartheta_R), \quad s_Z(\vartheta_Z) = -\vartheta_Z \log \vartheta_Z + \vartheta_Z(1 - \log \ell). \quad (\text{S47})$$

Analogously to the easy-axis case, the constant C is fixed by looking at the free energy in the infinite temperature limit

$$F = L \int_0^{\pi/\varrho_{\text{ep}}} \frac{d\sigma}{\sigma^2} \left(\min(\sigma, 1) - \sigma \frac{\varrho_{\text{ep}}}{\pi} \right) \left(1 - \frac{\mu^2 \sigma^2}{\sinh^2(\mu\sigma)} \right) + L \frac{\varrho_{\text{ep}}}{\pi} \log \left(\frac{\mu \ell e^{\ell\mu}}{\sinh(\ell\mu)} \right) - LC = L(\mu + \log(\mu/\sinh \mu) - C). \quad (\text{S48})$$

Hence, by consistency with the microscopic calculation, we ask $C = 0$. From the free energy, one can immediately derive the magnetization by noticing that $\langle M^3 - M_{\text{vac}}^3 \rangle = -\partial_\mu F$

The spin-waves limit.— The analysis of the spin-waves limit follows similar steps to those of the easy-axis. In Eqs. (S40)(S41)(S42) we consider μ to be large. In this limit, the filling function ϑ_Z is exponentially suppressed and can be entirely neglected. For the effective energy ε_σ , we can use the same approximation we made in the easy-axis regime and assume only small strings $\sigma \ll 1$ matter. In this limit we can replace $T_{\sigma, \sigma'}(\lambda) \simeq 2 \min(\sigma, \sigma') \delta(\lambda)$. Similarly

$T_{\sigma,R}(\lambda) = -2\sigma\ell\delta(\lambda)$, however, as one can check a posteriori, $\log \epsilon_R$ logarithmically diverges and this is negligible compared with the bare energy contribution in Eq. (S40). Hence, the strong-polarization approximation of Eq. (S40) is formally identical to Eq. (S29), with the only difference of computing $e^{(1)}(\lambda)$ in the easy-plane regime. In the TBA equations for radiation (S42), at the leading order one can approximate the effective energy with the bare source term $\vartheta_R(\lambda) = \frac{1}{\beta e_R(\lambda) + \mu m_R}$ and entirely neglect dressing effects.

We should now retrieve the thermodynamics of spin waves: these modes receive contributions both from the already existing radiative modes, and, similarly to the easy-axis regime, from the collective effect of the solitons, analogously to Eq. (S30). To this end, we define $\partial_\lambda p^{(1)}(\lambda) = \lim_{\sigma \rightarrow 0} \sigma^{-1} \partial_\lambda p_\sigma(\lambda)$ and $e^{(1)}(\lambda) = \lim_{\sigma \rightarrow 0} \sigma^{-1} e_\sigma(\lambda)$, and the two momentum branches

$$k_+(\lambda) = \int^\lambda \partial_{\lambda'} p^{(1)}(\lambda') = -2 \arctan[\coth \lambda \tan(\varrho_{\text{ep}}/2)]. \quad k_+ \in [-\pi, -\varrho_{\text{ep}}] \cup [\varrho_{\text{ep}}, \pi], \quad (\text{S49})$$

$$k_-(\lambda) = \int^\lambda \partial_{\lambda'} p_R(\lambda') = -2 \arctan[\tanh \lambda \tan(\varrho_{\text{ep}}/2)]. \quad k_- \in [-\varrho_{\text{ep}}, \varrho_{\text{ep}}]. \quad (\text{S50})$$

Together, the two branches k_+ and k_- cover the whole Brillouin zone. By inverting the above relation $\lambda_+(k)$ and $\lambda_-(k)$ one obtains the spin waves dispersion

$$e_{\text{SW}}(k) = \begin{cases} e^{(1)}(\lambda_+(k)) & k \in [-\pi, -\varrho_{\text{ep}}] \cup [\varrho_{\text{ep}}, \pi] \\ e_R(\lambda_-(k)) & k \in [-\varrho_{\text{ep}}, \varrho_{\text{ep}}] \end{cases} \Rightarrow e_{\text{SW}}(k) = \frac{4\varrho_{\text{ep}}}{\sin \varrho_{\text{ep}}} (\cos \varrho_{\text{ep}} - \cos k). \quad (\text{S51})$$

This result agrees with the spin-waves analysis of Section 2.

3. The isotropic limit

The isotropic point can be obtained as a limiting case of either the easy-axis, or easy-plane case. For the sake of simplicity, we consider the easy-axis and send the anisotropy to zero $\varrho_{\text{ea}} \rightarrow 0$. As it is clear from the scattering kernel (S19), a non-trivial limit can be obtained by rescaling the rapidities $\lambda \rightarrow \varrho_{\text{ea}} \lambda$ before taking the limit. The straightforward procedure leads to the TBA equations and Drude weight formally identical to Eqs. (S21) and (S23), but now the rapidity domain covers the whole real axis $\lambda \in [-\infty, \infty]$, the bare energy and momentum are $\partial_\lambda p_\sigma = \pi T_{\sigma,1}(\lambda)$ and $e_\sigma(\lambda) = 2\partial_\lambda p_\sigma(\lambda)$, while the scattering kernel at the isotropic point is

$$T_{\sigma,\sigma'}(\lambda) = \frac{1}{\pi} \log \left[\frac{\lambda^2 + \left(\frac{\sigma+\sigma'}{2}\right)^2}{\lambda^2 + \left(\frac{\sigma-\sigma'}{2}\right)^2} \right]. \quad (\text{S52})$$

We do not repeat the analysis of the infinite temperature and spin-waves limits, since they are analogue to the easy-axis case.

4. The continuum Landau-Lifschitz

We finally focus on the continuum limit of the classical spin chain Eq. (1). The continuum limit can be taken at the level of TBA: for this reason, we introduce a lattice spacing $a \rightarrow 0$. In the continuum limit of the lattice model, one needs to zoom on slow quasiparticles carrying large magnetization: in order to get non-trivial scattering kernels, the anisotropy should be rescaled accordingly. For the sake of convenience, we consider separately the easy-axis and the easy-plane regimes: the isotropic point is straightforwardly obtained as a limiting case of the easy-axis regime.

The easy-axis regime.— We consider the following rescaling. We introduce a label “c” for those quantities that describe the continuum model

$$\varrho_{\text{ea}} = a\varrho_{\text{ea};c}, \quad \sigma = \sigma_c/a, \quad e_\sigma(\lambda) = a e_{c;\sigma_c}(\lambda), \quad T_{\sigma,\sigma'}(\lambda) = \frac{1}{a} T_{c;\sigma_c,\sigma'_c}(\lambda) \quad (\text{S53})$$

Likewise, the temperature and chemical potential needs to be properly rescaled as $\beta = a^{-1}\beta_c$ and $\mu = a\mu_c$. The rapidity is not rescaled, and it still has values in the compact domain $\lambda \in [-\pi/2, \pi/2]$.

The $a \rightarrow 0$ limit can be safely taken, leading to the same form of the TBA equations and Drude weight as in the lattice version, provided the scattering kernels and dispersion laws are replaced with the continuum counterparts

$$\partial_\lambda p_{c;\sigma_c}(\lambda) = \frac{2 \sinh(\varrho_{\text{ea};c} \sigma_c)}{\cosh(\varrho_{\text{ea};c} \sigma_c) - \cos(2\lambda)}, \quad T_{c;\sigma_c,\sigma'_c}(\lambda) = \frac{1}{\pi \varrho_{\text{ea};c}} \log \left(\frac{\cosh((\sigma_c + \sigma'_c) \varrho_{\text{ea};c}) - \cos(2\lambda)}{\cosh((\sigma_c - \sigma'_c) \varrho_{\text{ea};c}) - \cos(2\lambda)} \right), \quad (\text{S54})$$

while the magnetization eigenvalue retains the same form $m_{c;\sigma_c} = 2\sigma_c$ and the energy $e_{c,\sigma_c} = 2\varrho_{\text{ea};c} \partial_\lambda p_{c;\sigma_c}(\lambda)$. Notice that, in the continuum limit, the modes with divergent bare energy are now at $\sigma_c = 0$ and $\lambda = 0$. By taking the continuum limit directly at the level of the spin-waves analysis of the lattice model in Section 2, and comparing with the spin-waves analysis of the continuum Hamiltonian, one can identify $\Delta = \varrho_{\text{ea};c}^2$.

The easy-plane regime.— In the continuum limit, the easy-plane features the same excitations that are also present in the lattice and the rapidity still covers the whole real axis $\lambda \in (-\infty, \infty)$. As in the easy-axis regime, we introduce a lattice spacing a and the following rescaling

$$\varrho_{\text{ep}} = a \varrho_{\text{ep};c}, \quad \sigma = \sigma_c / a, \quad e_\sigma(\lambda) = a e_{c;\sigma_c}(\lambda), \quad e_R(\lambda) = a e_{c;R}(\lambda) \quad (\text{S55})$$

$$T_{\sigma,\sigma'}(\lambda) = \frac{1}{a} T_{c;\sigma_c,\sigma'_c}(\lambda), \quad T_{\sigma,R}(\lambda) = \frac{1}{a} T_{c;\sigma_c,R}(\lambda), \quad T_{R,R}(\lambda) = a T_{c;R,R}(\lambda), \quad T_{Z,R}(\lambda) = T_{c;Z,R}(\lambda) \quad (\text{S56})$$

It is also useful to introduce $\ell_c = \pi / \varrho_{\text{ep};c}$: notice that, due to the rescaling, $\sigma_c \in [0, \ell_c]$. Taking the continuum limit $a \rightarrow 0$ one formally obtains the same TBA equations of the planar regime on the lattice, provided the continuum dispersion law and scattering kernels are used

$$\partial_\lambda p_{c;\sigma_c}(\lambda) = \frac{2 \sin(\varrho_{\text{ep};c} \sigma_c)}{\cosh(2\lambda) - \cos(\varrho_{\text{ep};c} \sigma_c)}, \quad \partial_\lambda p_{c;R}(\lambda) = -\frac{2 \varrho_{\text{ep};c}}{\cosh(2\lambda) + \cos(\varrho_{\text{ep};c} \sigma_c)} \quad (\text{S57})$$

and $\partial_\lambda p_{c;Z}(\lambda) = 0$, the energies are $e_{c,\sigma_c}(\lambda) = 2 \varrho_{\text{ep};c} \partial_\lambda p_{c;\sigma_c}(\lambda)$, $e_{c,R}(\lambda) = 2 \varrho_{\text{ea};c} \partial_\lambda p_{c;R}(\lambda)$ and $e_{c;Z}(\lambda) = 0$. The magnetization eigenvalue reads $m_{c;\sigma_c} = 2\sigma_c$, $m_{c;R} = 2$ and $m_{c;Z} = 2\ell_c$. Finally, the kernels are read from Eq. (S56). From the spin-waves limit, we can identify $\Delta = -\varrho_{\text{ep};c}^2$.

4. NUMERICAL METHODS

In this section we provide a short account for the numerical methods we use, more precisely we describe the numerical discretization of the TBA in Section 4.1 and a short description of the Monte Carlo simulations in Section 4.2. Working Mathematica notebooks for the numerical solution of the TBA and computation of the Drude weight are provided on Zenodo [113].

1. Solving the TBA equations

For the sake of simplicity, we describe the discretization in the easy-axis case: the easy-plane regime is analogous. The numerical solution of the TBA equations needs to correctly account for two different singularities: the first happens at small σ and arbitrary rapidities λ , where the filling function diverges as $\sim 1/\sigma^2$, the second is placed around $(\sigma, \lambda) = (1, 0)$, where the bare energy and momentum become singular. The first problem can be solved with a convenient reparametrization of the filling functions and dressing equations, along the lines of previous works on the focusing nonlinear Schrödinger [84] and sine-Gordon [85] models. To this end, we define $\bar{\vartheta}_\sigma(\lambda) = \sigma^2 \vartheta_\sigma(\lambda)$ and a new dressing operation that we denote as “bold dressing” $(\dots)^{\text{dr}}$ such that $\sigma^2 (g_\sigma)^{\text{dr}} = g_\sigma^{\text{dr}}$. The new dressing operation can be recasted as the following linear equation

$$\sigma g_\sigma^{\text{dr}}(\lambda) = \sigma^{-1} g_\sigma(\lambda) - \sigma^{-1} \int_0^\infty d\sigma' \int_{-\pi/2}^{\pi/2} d\lambda' T_{\sigma,\sigma'}(\lambda - \lambda') \bar{\vartheta}_{\sigma'}(\lambda') g_{\sigma'}^{\text{dr}}(\lambda'). \quad (\text{S58})$$

For those bare functions $g_\sigma(\lambda)$ that linearly vanish at small σ , i.e. $g_\sigma(\lambda) \propto \sigma$ (like it happens for the magnetization, energy, momentum and their derivatives), the new dressing is smooth (due to the fact that also $T_{\sigma,\sigma'}(\lambda)$ vanishes as $\propto \sigma$). As a great advantage, in the new parametrization $\vartheta_{\sigma'} g_{\sigma'}^{\text{dr}}(\lambda')$ is smooth and Eq. (S60) is easier to discretize.

Notice also that, very conveniently, $\rho_\sigma(\lambda) = \frac{1}{2\pi} \vartheta_\sigma(\partial_\lambda p_\sigma)^{\text{dr}} = \frac{1}{2\pi} \bar{\vartheta}_\sigma(\partial_\lambda p_\sigma)^{\text{dr}}$. For what concerns the determination of the filling functions on thermal states, we use the parametrization of the filling function in terms of the effective energy $\varepsilon_\sigma(\lambda)$ according to Eq. (S21): the effective energy can be considered a smooth function in the discretization. We now approximate the integral equations with matrix-vector equations by building a grid in the (σ, λ) space. In particular, we consider an independent cartesian discretization $\{\lambda_j\}_{j=1}^{N_\lambda} \otimes \{\sigma_i\}_{i=1}^{N_\sigma}$ where each point represent the edge of a small integration interval. It is important that rapidities are discretized independently from σ to capture the asymptotic behavior of the scattering kernel $\lim_{\sigma, \sigma' \rightarrow 0} T_{\sigma, \sigma'}(\lambda) \propto \delta(\lambda)$. The discretizations $\{\lambda_j\}_{j=1}^{N_\lambda}$ and $\{\sigma_i\}_{i=1}^{N_\sigma}$ are non-uniform in space to better capture the dangerous points. Hence, $\{\sigma_i\}_{i=1}^{N_\sigma}$ is denser around zero and one, while $\{\lambda_j\}_{j=1}^{N_\lambda}$ is denser around zero. We then discretize the filling as

$$\bar{\vartheta}_\sigma(\lambda) \rightarrow \bar{\vartheta}(i, j) = \bar{\vartheta}_{\frac{1}{2}(\sigma_i + \sigma_{i+1})} \left(\frac{\lambda_j + \lambda_{j+1}}{2} \right) \quad (\text{S59})$$

and similarly for the other functions, which are now seen as a vector in the (i, j) space with dimension $(N_\lambda - 1) \times (N_\sigma - 1)$. The dressing equation (S60) (and similarly the TBA (S21)) becomes a matrix equation as

$$g^{\text{dr}}(i, j) = \left(\frac{\sigma_i + \sigma_{i+1}}{2} \right)^{-1} g_{\frac{\sigma_i + \sigma_{i+1}}{2}} \left(\frac{\lambda_j + \lambda_{j+1}}{2} \right) - \left(\frac{\sigma_i + \sigma_{i+1}}{2} \right)^{-1} \sum_{(i', j')} T[(i, j), (i', j')] \bar{\vartheta}(i', j') g^{\text{dr}}(i', j'). \quad (\text{S60})$$

Ideally, we define the discretized kernel as

$$T[(i, j), (i', j')] = \int_{\sigma_{i'}}^{\sigma_{i'+1}} d\sigma \int_{\lambda_{j'}}^{\lambda_{j'+1}} d\lambda T_{\frac{\sigma_i + \sigma_{i+1}}{2}, \sigma} \left(\frac{\lambda_j + \lambda_{j+1}}{2} - \lambda \right), \quad (\text{S61})$$

but we approximate the integral by correctly accounting for the singular behavior of the kernel. In the easy-axis regime, we define the singular part of the kernel

$$T_{\sigma, \sigma'}^{\text{Sing}}(\lambda) = \frac{1}{\pi \varrho_{\text{ea}}} \cos(\lambda) \log \left[\frac{(\sigma + \sigma')^2 \varrho_{\text{ea}}^2 + 4 \sin^2(\lambda)}{(\sigma - \sigma')^2 \varrho_{\text{ea}}^2 + 4 \sin^2(\lambda)} \right], \quad (\text{S62})$$

while the non-singular part is defined as the reminder $T_{\sigma, \sigma'}^{\text{NSing}}(\lambda) = T_{\sigma, \sigma'}(\lambda) - T_{\sigma, \sigma'}^{\text{Sing}}(\lambda)$. The singular part of the kernel has the following important features: *i*) it captures all the singularities of $T_{\sigma, \sigma'}(\lambda)$, thus leaving $T_{\sigma, \sigma'}^{\text{NSing}}(\lambda)$ a smooth function, *ii*) it has the correct periodicity over λ and the correct asymptotics for small σ , i.e. $\lim_{\sigma \rightarrow 0} T_{\sigma, \sigma'}^{\text{Sing}}(\lambda) = 0$, *iii*) and finally it can be easily analytically integrated over both strings and rapidities. Therefore, in the definition of the discretized kernels (S61), we perform exactly the integral over the singular part and approximate by the midpoint rule the integration over the non-singular term

$$T[(i, j), (i', j')] \simeq (\sigma_{i'+1} - \sigma_{i'}) (\lambda_{j'+1} - \lambda_{j'}) T_{\frac{\sigma_i + \sigma_{i+1}}{2}, \frac{\sigma_{i'} + \sigma_{i'+1}}{2}}^{\text{NSing}} \left(\frac{\lambda_j + \lambda_{j+1}}{2} - \frac{\lambda_{j'} + \lambda_{j'+1}}{2} \right) + \int_{\sigma_i}^{\sigma_{i+1}} d\sigma \int_{\lambda_j}^{\lambda_{j+1}} d\lambda T_{\frac{\sigma_i + \sigma_{i+1}}{2}, \sigma}^{\text{Sing}} \left(\frac{\lambda_j + \lambda_{j+1}}{2} - \lambda \right). \quad (\text{S63})$$

With this discretization, the TBA equations are convergent and correctly reproduce the known limiting case (high temperature and small magnetization), and give results in agreement with numerical simulations. So far, we left pending the problem of the singularity in the bare energy and momentum at $(\sigma, \lambda) = (1, 0)$, which must be carefully handled when computing the Drude weight. As an example, we focus on the dressed energy derivative $(\partial_\lambda e_\sigma)^{\text{dr}}$: the same analysis must be done for the dressed momentum derivative $(\partial_\lambda p_\sigma)^{\text{dr}}$ and the effective energy ε_σ which parametrizes the filling. We notice that the singularity in $(\partial_\lambda e_\sigma)^{\text{dr}}$ is due to the bare term. It is thus convenient to define $(\partial_\lambda e_\sigma)^{\text{dr, NSing}} = (\partial_\lambda e_\sigma)^{\text{dr}} - \sigma^{-2} \partial_\lambda e_\sigma - \sigma^{-1} \partial_\lambda e^{(1)}$, where we recall the definition $e^{(1)}(\lambda) = \lim_{\sigma \rightarrow 0} \sigma^{-1} e_\sigma(\lambda)$: with this definition, $(\partial_\lambda e_\sigma)^{\text{dr, NSing}}$ is smooth everywhere and goes to a constant for $\sigma \rightarrow 0$. Hence, from the numerical solution of the dressing equation, we compute the discretized version of $(\partial_\lambda e_\sigma)^{\text{dr, NSing}}$ and interpolate it: in this way, $(\partial_\lambda e_\sigma)^{\text{dr}}$ is split in a singular part that we analytically control and a non-singular part that comes from the interpolation. This expression and the analogue for $(\partial_\lambda p_\sigma)$ and ε_σ are then plug into the integral expression for the Drude weight. In this case, a change of variables from (σ, λ) to (σ, E) is convenient, where we define $E = e_\sigma(\lambda)$: as we discussed when extracting the large temperature asymptotics of \mathcal{D} , the singularity of the dressed velocity is now placed at $E \rightarrow \infty$. In this space, we perform the integral first in the σ axis at fixed E , and sample the curve up

to an energy cutoff E_c which is chosen in such a way it correctly reproduces the asymptotic form Eq. (S25). Then, the curve is interpolated and numerically integrated up to $E < E_c$, while the tail $E > E_c$ is integrated analytically. This method gives convergent results which are reliable even in the large temperature limit. A similar procedure is used for the easy-plane regime as well. On Zenodo [113], we provide commented Mathematica notebooks where this numerical scheme is implemented in practice.

2. Microscopic simulations

The microscopic simulations consist in two steps: *i*) sampling initial configurations from thermal ensemble using a Metropolis-Hasting method, and *ii*) evolving each initial condition with a deterministic dynamics, computing the evolution of the spin current. The Drude weight is then computed by averaging over initial configurations. In what follows we discuss each of these steps in details.

Monte-Carlo sampling

We consider equilibrium ensembles

$$\rho_L(\beta, \mu) = \mathcal{Z}_L^{-1} e^{-\beta H + \mu M^3}, \quad (\text{S64})$$

where $M^3 = \sum_{\ell=1}^L S_\ell^3$ is the total magnetization and

$$\mathcal{Z}_L = \int d\Omega^{\times L} e^{-\beta H + \mu M^3} \quad (\text{S65})$$

is the partition function with the uniform measure $d\Omega^{\times L} = \prod_{\ell=1}^L d\Omega_\ell$. The expectation value of an observable $\mathcal{O}_\ell(t)$ in the ensemble (S64) is given by

$$\langle \mathcal{O}_\ell(t) \rangle = \int d\Omega^{\times L} \mathcal{O}_\ell(t) \rho_L(\beta, \mu). \quad (\text{S66})$$

The ensemble (S64) is efficiently sampled by an implementation of the Monte-Carlo method:

1. Sample an initial spin configuration $\{\mathbf{S}\} = \{\mathbf{S}_\ell\}_{\ell=1}^L$ from the uniform measure $d\Omega^{\times L}$.
2. Compute the energy $H(\{\mathbf{S}\})$ and magnetization $M^3(\{\mathbf{S}\})$ of the spin configuration.
3. Pick a random lattice site $1 \leq j \leq L$ and sample a random direction \mathbf{N} from the uniform measure $d\Omega$.
4. Generate an alternative spin $\mathbf{S}'_j = \mathbf{S}_j \cos \theta + (\mathbf{N} \times \mathbf{S}_j) \sin \theta + \mathbf{N}(\mathbf{N} \cdot \mathbf{S}_j)(1 - \cos \theta)$ where $\theta \ll 1$.
5. Construct an alternative spin configuration $\{\mathbf{S}'\} = \{\mathbf{S}_\ell\}_{\ell=1}^{j-1} \cup \{\mathbf{S}'_j\} \cup \{\mathbf{S}_\ell\}_{\ell=j+1}^L$.
6. Compute the changes of energy $\delta H = H(\{\mathbf{S}'\}) - H(\{\mathbf{S}\})$ and magnetization $\delta M^3 = M^3(\{\mathbf{S}'\}) - M^3(\{\mathbf{S}\})$ of the alternative spin configuration relative to the unperturbed spin configuration.
7. Update the spin configuration $\{\mathbf{S}\} \leftarrow \{\mathbf{S}'\}$ with probability $p = \min\{1, e^{-\beta \delta H + \mu \delta M^3}\}$.
8. Repeat steps 3-7 until satisfactory convergence is obtained.

Note that while the ensemble (S64) is an invariant measure for the continuous-time dynamics Φ (S67), it is not an invariant measure for the discrete-time dynamics Φ_τ (S68) for $\tau > 0$ (see below). Our use of the continuous-time ensemble for the discrete-time dynamics makes the initial state effectively a non-equilibrium ensemble. However, we have verified that the resulting deviations from continuous-time dynamics at the used value of τ are within the estimated uncertainty interval.

Time-evolution

The evolution $\Phi : (\mathcal{S}^2)^{\times L} \rightarrow (\mathcal{S}^2)^{\times L}$ generated by the Hamiltonian (2) that maps the spins forwards in time

$$\{\mathbf{S}_\ell(t + t_0)\}_{\ell=1}^L = \Phi(t) [\{\mathbf{S}_\ell(t_0)\}_{\ell=1}^L]. \quad (\text{S67})$$

is integrable, indeed it conserves an extensive tower of charges $\{Q_n\}_{n=1}^L$, the first one being the Hamiltonian $Q_1 \simeq H$. To avoid breaking its integrability by a direct time discretization, we instead use a discretization developed in [61] that preserves integrability by construction. The discrete-time evolution map $\Phi_\tau : (\mathcal{S}^2)^{\times L} \rightarrow (\mathcal{S}^2)^{\times L}$

$$\{\mathbf{S}_\ell(T + T_0)\}_{\ell=1}^L = \Phi_\tau(T) [\{\mathbf{S}_\ell(T_0)\}_{\ell=1}^L], \quad (\text{S68})$$

depends on a time-step parameter $\tau \in \mathbb{R}$. Hamiltonian dynamics are recovered in the continuous-time limit

$$\lim_{\substack{\tau \rightarrow 0, T \rightarrow \infty \\ T\tau = t}} \Phi_\tau(T) = \Phi(t). \quad (\text{S69})$$

The discrete-time map Φ_τ conserves an extensive tower of τ -deformed charges $\{Q_n^{(\tau)}\}_{n=1}^L$ that reduce to their continuum-time counterparts, $\lim_{\tau \rightarrow 0} \{Q_n^{(\tau)}\}_{n=1}^L = \{Q_n\}_{n=1}^L$. All reported simulations use the value $\tau = 0.03$ and are terminated before periodicity of the finite size of the system is manifest, $T_{\max} < L/2$. While the estimated values of dynamical quantities depend on the time-step parameter τ , we have verified that results for smaller values of τ are contained within the estimated uncertainty interval.

Expectation values

We estimate expectation values (S66) by averaging over N samples drawn from the ensemble (S64)

$$\overline{\mathcal{O}_\ell(t)} = N^{-1} \sum_{n=1}^N \mathcal{O}_\ell^{[n]}(t), \quad (\text{S70})$$

where $\bullet^{[n]}$ denotes evaluation in the n -th sample. Uncertainty of the estimate (S70) is extracted from the standard deviation of the samples

$$\sigma_{\mathcal{O}_\ell(t)}^2 = N^{-1} \sum_{n=1}^N [\mathcal{O}_\ell^{[n]}(t) - \langle \mathcal{O}_\ell(t) \rangle]^2. \quad (\text{S71})$$

Since samples in Eq. (S70) are independent, it follows by the central limit theorem that as the number of samples N grows, the distribution of the average $\overline{\mathcal{O}_\ell(t)}$ approaches a Gaussian distribution centered at $\langle \mathcal{O}_\ell(t) \rangle$ with standard deviation

$$\sigma_{\overline{\mathcal{O}}} = N^{-1/2} \sigma_{\mathcal{O}}, \quad (\text{S72})$$

which gives the uncertainty interval (with standard score $z = 1$) of the estimated average value

$$\langle \mathcal{O}_\ell(t) \rangle \approx \overline{\mathcal{O}_\ell(t)} \pm \sigma_{\overline{\mathcal{O}}}. \quad (\text{S73})$$

We extract the spin Drude weight using the Green-Kubo identity. We work in the continuous-time setting, the adaptation to the discrete-time setting is straightforward, see Ref. [61] for details. Spin satisfies a continuity equation

$$\partial_t S_\ell^3(t) + j_{\ell+1}(t) - j_\ell(t) = 0, \quad (\text{S74})$$

where j_ℓ is the spin current density. We define the total spin current as

$$J(t) = \sum_{\ell=1}^L j_\ell(t). \quad (\text{S75})$$

The finite-time finite-size Drude weight is given by the integral of the total spin current auto-correlation function

$$\mathcal{D}_L(t) = t^{-1} L^{-1} \int_0^t dt \langle J(t) J(0) \rangle^c, \quad (\text{S76})$$

where $\langle XY \rangle^c = \langle XY \rangle - \langle X \rangle \langle Y \rangle$ denotes the connected part of the correlation function. The Drude weight then correspond to the thermodynamic value of the long-time limit of (S76)

$$\mathcal{D} = \lim_{t \rightarrow \infty} \lim_{L \rightarrow \infty} \mathcal{D}_L(t). \quad (\text{S77})$$